

available at www.sciencedirect.com

SciVerse ScienceDirect

www.elsevier.com/locate/molonc

VGLL3 expression is associated with a tumor suppressor phenotype in epithelial ovarian cancer

Karen Gambaro^a, Michael C.J. Quinn^{b,1}, Paulina M. Wojnarowicz^{a,1},
Suzanna L. Arcand^c, Manon de Ladurantaye^b, Véronique Barrès^b,
Jean-Sébastien Ripeau^c, Ann M. Killary^d, Elaine C. Davis^e,
Josée Lavoie^{a,f}, Diane M. Provencher^{b,g}, Anne-Marie Mes-Masson^{b,h},
Mario Chevette^{c,i}, Patricia N. Tonin^{a,c,j,*}

^aDepartment of Human Genetics, McGill University, Montreal General Hospital, 1650 Cedar Avenue, Montreal H3G 1A4, Quebec, Canada

^bCentre de recherche du Centre hospitalier de l'Université de Montréal, Institut du cancer de Montréal, 1560 rue Sherbrooke est, Montreal H2L 4M1, Canada

^cThe Research Institute of McGill University Health Centre, Montreal General Hospital, 1650 Cedar Avenue, Montreal H3G 1A4, Canada

^dDepartment of Genetics, The University of Texas M.D. Anderson Cancer Center, 1515 Holcombe Blvd., Houston, 77030 TX, USA

^eDepartment of Anatomy and Cell Biology, McGill University, 3640 rue University, Montreal H3A 0C7, Canada

^fDepartment of Pathology, McGill University, Montreal Children's Hospital, 2300 Tupper Street, H3H 1P3 Montreal, Canada

^gDivision de gynécologie oncologique, Université de Montréal, 1560 rue Sherbrooke est, H2L 4M1 Montreal, Canada

^hDepartment de Médecine, Université de Montréal, 1560 rue Sherbrooke est, H2L 4M1 Montreal, Canada

ⁱDepartment of Surgery, Urology Division, McGill University, Montreal General Hospital, 1650 Cedar Avenue, H3G 1A4 Montreal, Canada

^jDepartment of Medicine, McGill University, Montreal General Hospital, 1650 Cedar Avenue, H3G 1A4 Montreal, Canada

ARTICLE INFO

Article history:

Received 12 November 2012

Received in revised form

14 December 2012

Accepted 20 December 2012

Available online 16 January 2013

Keywords:

High-grade ovarian serous

ABSTRACT

Previous studies have implicated *vestigial like 3* (*VGLL3*), a chromosome 3p12.3 gene that encodes a putative transcription co-factor, as a candidate tumor suppressor gene (TSG) in high-grade serous ovarian carcinomas (HGSC), the most common type of epithelial ovarian cancer. A complementation analysis based on microcell-mediated chromosome transfer (MMCT) using a centric fragment of chromosome 3 (der3p12-q12.1) into the OV-90 ovarian cancer cell line haploinsufficient for 3p and lacking *VGLL3* expression was performed to assess the effect on tumorigenic potential and growth characteristics. Genetic characterization of the derived MMCT hybrids revealed that only the hybrid that contained an intact *VGLL3* locus exhibited alterations of tumorigenic potential in a nude mouse xenograft

Abbreviations: HGSC, high-grade serous carcinomas; MMCT, microcell-mediated chromosome transfer; MVB, multivesicular-bodies; TSG, tumor suppressor gene; chr, chromosome; s.c., sub-cutaneous; i.p., intraperitoneal.

* Corresponding author. Department of Human Genetics, McGill University, Medical Genetics, Room L10-132, Montreal General Hospital, 1650 Cedar Avenue, Montreal H3G 1A4, Quebec, Canada. Tel.: +1 514 934 1934x44069; fax: +1 514 934 8273.

E-mail address: patricia.tonin@mcgill.ca (P.N. Tonin).

¹ Authors contributed equally to this work.

1574-7891/\$ – see front matter © 2013 Federation of European Biochemical Societies. Published by Elsevier B.V. All rights reserved.

<http://dx.doi.org/10.1016/j.molonc.2012.12.006>

carcinomas
 Microcell-mediated chromosome
 transfer
 VGLL3
 Tumor suppressor gene
 Chromosome 3
 3p12
 Gene transfection
 Gene expression

model and various *in vitro* growth characteristics. Only stable OV-90 transfectant clones expressing low levels of VGLL3 were derived. These clones exhibited an altered cytoplasmic morphology characterized by numerous single membrane bound multivesicular-bodies (MVB) that were not attributed to autophagy. Overexpression of VGLL3 in OV-90 was achieved using a lentivirus-based tetracycline inducible gene expression system, which also resulted in MVB formation in the infected cell population. Though there was no significant differences in various *in vitro* and *in vivo* growth characteristics in a comparison of VGLL3-expressing clones with empty vector transfectant controls, loss of VGLL3 expression was observed in tumors derived from mouse xenograft models. VGLL3 gene and protein expression was significantly reduced in HGSC samples (>98%, $p < 0.05$) relative to either normal ovarian surface epithelial cells or epithelial cells of the fallopian tube, possible tissues of origin of HGSC. Also, there appeared to be more cases with higher staining levels in stromal tissue component from HGSC cases that had a prolonged disease-free survival. The results taken together suggest that VGLL3 is involved in tumor suppressor pathways, a feature that is characterized by the absence of VGLL3 expression in HGSC samples.

© 2013 Federation of European Biochemical Societies.

Published by Elsevier B.V. All rights reserved.

1. Introduction

Ovarian cancer is the fifth leading cause of cancer-related deaths in women in the developed world, where high-grade ovarian serous carcinomas (HGSC) account for the majority of all epithelial ovarian cancer cases (Chen et al., 2003; Seidman et al., 2004). Though highly responsive to the standard of care involving cytoreductive surgery and platinum-taxane chemotherapy, overall survival is less than 30% and this has been attributed to advanced stage at diagnosis, repeated recurrences, and the development of drug resistance for the majority of HGSC cases (Aletti et al., 2007). Thus, elucidating the factors important in the development and progression of HGSC has been a major focus of research in order to develop more effective treatment strategies. Though HGSCs share in common a high frequency (>90%) of TP53 mutations and a highly disorganized genome with common chromosomal (chr) anomalies (Ahmed et al., 2010; Gorringer and Campbell, 2009; Singer et al., 2005; Wojnarowicz et al., 2012b), significant heterogeneity exists suggesting that they may develop through different molecular pathways. Our research group has been interested in investigating the possibility that the short arm (p) of chr 3 harbors tumor suppressor genes (TSG) important in ovarian cancer as suggested by loss of heterozygosity (LOH) studies (Lounis et al., 1998; Manderson et al., 2002). As more than one 3p interval was identified by LOH analyses (Lounis et al., 1998), we applied a genetic complementation approach to guide our search and gather further functional evidence in support of 3p TSGs. Through the transfer of normal chr 3 fragments into the OV-90 ovarian cancer cell line, our group identified 3p14-pcen as a candidate TSG containing region (Cody et al., 2007, 2009). We used the tumorigenic OV-90 cell line as model for our studies as this cell line is haploinsufficient for 3p and exhibits all of the major features of HGSCs such as a TP53 mutation and chr anomalies (Provencher et al., 2000). OV-90 is tumorigenic in mouse xenograft models with ascites formation at intraperitoneal sites, and is able to form colonies in soft agarose and spheroids in hanging drop cultures (Cody et al., 2007; Provencher et al., 2000). It is these *in vivo* and *in vitro* growth characteristics that were abrogated

in our OV-90 hybrids containing normal chr 3p fragments (Cody et al., 2007). Whole genome transcriptome analyses, which also included an interrogation of data from HGSC transcriptomes, suggested that molecular networks characteristic of HGSC had been affected in these non-tumorigenic hybrids (Cody et al., 2009; Quinn et al., 2009a). Though 3p14-pcen contains a number of plausible TSGs, molecular genetic analyses ranked VGLL3 at 3p12.3 as a top candidate to pursue based on comparative gene expression profiles of HGSCs and various ovarian cancer cell lines that differed in their tumorigenic potential (Cody et al., 2007, 2009).

VGLL3 overlaps an anonymous cDNA clone (AF099505) that was identified using the technique of mRNA differential display of colorectal cancers, and thus originally referred to as “colon carcinoma related protein” gene (Wang et al., 1999). VGLL3 cDNA was subsequently identified in placental tissues by similarity to the transcription enhancer 1 (TEAD1) interaction domain (Maeda et al., 2002). In *Drosophila*, the TEAD homolog, *scalloped* (Sg) interacts with the co-factor *vestigial* (Vg) to drive differentiation of wings and indirect flight muscles (Legend et al., 2006). Other than our initial gene expression analysis in ovarian cancer related model systems, which showed low or absent VGLL3 expression in HGSC relative to normal cells (Birch et al., 2008; Cody et al., 2007, 2009; Quinn et al., 2009a), the mammalian ortholog has not been investigated.

In this report, we began our analyses with functional gene complementation assays using a microcell-mediated chromosome transfer (MMCT) technique with a unique derivative chr 3, der3p12-q11, which has been shown to suppress the tumorigenic potential of renal cell carcinoma cell lines in MMCT assays (Lott et al., 1998). We describe the results of our analyses of the MMCT hybrids, which reaffirmed VGLL3 as a top candidate to pursue. Then we describe the targeted analysis of VGLL3 in the context of cell transfection assays, where most notably expression was lost in tumors resulting from mouse xenograft models. We also describe an unusual cytoplasmic phenotype characterized by presence of numerous single membrane bound multivesicular-bodies (MVB) found only in VGLL3 transfectant clones and cells expressing VGLL3 using an inducible lentiviral system. Finally, we relate VGLL3 protein expression

to clinical parameters and demonstrate absent or low levels of VGLL3 expression in cancer specimens relative to normal tissues and a trend toward an improved progression-free survival outcome in patients exhibiting evidence of VGLL3 expression in the stromal compartment of the tumor.

2. Materials and methods

2.1. MMCT of *der3p12-q11*

The MMCT assays were performed using a modified method (Killary et al., 1992). Briefly, the mouse-human hybrid HA(3) Ilaa cells containing a derivative of human chr 3, *der3p12-q12.1* tagged with pSV2neo (Lott et al., 1998; Sanchez et al., 1994), were incubated 48-h in colcemid at 0.06 $\mu\text{g/ml}$ to induce micronucleation. Enucleation of micronucleate populations was achieved using 10 $\mu\text{g/ml}$ cytochalasin B and centrifugation at $27,000 \times g$ for 30 min (28–32 °C). Microcell populations were enriched upon filtration through 5- and 3- μm nucleopore filters. Microcells were then resuspended with phytohemagglutinin P and added to a monolayer of the recipient cells, the human OV-90 ovarian cancer cell line haploinsufficient for 3p (Provencher et al., 2000), in a 25-cm² flask for 15–20-min at 37 °C. One ml of 50% polyethylene glycol (PEG 1500) was added as a fusing agent for 90 s. The MMCT hybrids were selected in OSE complete medium (Wisent Inc., St-Bruno, QC, Canada) containing 800 $\mu\text{g/ml}$ of G418 (Wisent Inc). Four microcell hybrid clones, OVHA3-1, OVHA3-2, OVHA3-3 and OVHA3-4 were derived from this fusion and maintained and expanded in G418 containing medium for further analysis. The hybrids were assessed for both mouse chr and *der3p12-q11* content by fluorescent *in situ* hybridization (FISH) analysis as described in Figure S1.

2.2. Genotyping analyses

PCR-based genotyping assays were performed as previously described (Cody et al., 2009) using polymorphic microsatellite markers and conditions described in Table S1. Genotyping was also performed using the Infinium™ HumanHap610 genotyping BeadChip technology (Illumina Inc., San Diego, CA, USA) as described previously (Birch et al., 2011), which contained 1544 markers mapping to 3p12-pcen. Genotyping and imaging using the BeadStudio Data Analysis software (Illumina Inc.) were performed at the McGill University and Genome Quebec Innovation Centre (Montreal, QC). The map coordinates were determined using the Feb. 2009 GRCh7/hg19 assembly of the human reference sequence (genome.ucsc.edu/cgi-bin/hgGateway).

2.3. Spheroid formation, soft agar and clonogenic assays

The capacity to form spheroids in hanging drop cultures and the ability to grow in anchorage independent conditions in soft agar were assessed as previously described (Cody et al., 2007; Zietarska et al., 2007). Clonogenic assays were performed with 500 cells seeded per well in a six-well plate, and allowed to grow for a period of about two weeks. Media was removed, cells washed with PBS and fixed in methanol. Post-fixation, the cells

were stained with Giemsa stain modified solution overnight (Sigma–Aldrich, Oakville, ON, Canada) and colonies counted. The surface area of the colonies were measured and the total surface area calculated for each well in the six-well plate for each experiment using ImageJ software version IJ 1.46r (Schneider et al., 2012). Differences in the area measure between groups were assessed by a student's t-test using Simple Interactive Statistical Analysis (<http://www.quantitative-skills.com/sisa/>). All assays were performed in triplicate.

2.4. Tumorigenicity assays

The tumorigenic potential of the cell lines was assessed based on their ability to form tumors in 42 day-old female SCID CB17 mice (Charles River Laboratories, Saint-Constant, QC, Canada) at subcutaneous (s.c.) left gluteal ($n = 6$ mice) and intraperitoneal (i.p.) injection sites ($n = 6$ mice). Each mouse was injected at the s.c. site with 1×10^6 cells suspended in a mix of 1:1 PBS and matrigel (BD Biosciences, Mississauga, ON, Canada) or at the i.p. site with 1×10^6 cells suspended PBS. Mice were also injected with PBS ($n = 4$, for each site). Data on weight of the mice and tumor dimensions (for s.c. experiments) were measured twice a week. Animals were housed under sterile conditions with *ad-lib* access to food and water. Animals were sacrificed and tumors collected before neoplastic masses reached greater than 2500 mm³ occurring at s.c. sites, or maximal tumor burden and ascites formation occurring at i.p. sites, according to the guidelines of the Canadian Council on Animal Care. Differences in the kinetics of tumor growth were assessed by Mann–Whitney *U*-test for s.c. experiments. A Kaplan–Meier survival curve analysis was performed for the i.p. experiment. Survival measured as the time to sacrifice for both s.c. and i.p. experiments was also evaluated by an one-way Anova with Tukey's *post hoc* test. All statistical tests were performed using SPSS software (Statistical Product and Service Solution Package, SPSS, 16.0).

2.5. VGLL3 expression analysis in cell lines and tumor xenografts

Gene expression analysis was performed from cDNA prepared from total RNA from cell lines, frozen tumor xenografts or HGSC samples by RT-PCR analyses essentially as described (Cody et al., 2007; Presneau et al., 2003). VGLL3 expression was also assessed by Real-Time RT-PCR using SYBR-Green PCR Master Mix (Qiagen Inc., Toronto, ON, Canada) on a Rotor-gene 3000 Real-Time Centrifugal DNA Amplification System (Corbett Research, Montreal Biotech Inc., Dorval, QC, Canada) according to the manufacturer's instructions. The cDNA samples were diluted 1:25 in water and 5 μl of the dilution were mixed with 10 pg of primers and 12.5 μl QuantiFast SYBR® Green PCR kit (Qiagen) for a final volume of 25 μl . The relative amount of VGLL3 to ERK-1 (control) and the fold stimulation was calculated by using equation (2)^{- $\Delta\Delta\text{CT}$} , where $\Delta\text{CT} = \text{CT}_{\text{VGLL3}} - \text{CT}_{\text{ERK1}}$ and $\Delta\Delta\text{CT} = \Delta\text{CT}_{\text{samples}} - \Delta\text{CT}_{\text{OV-90}}$. The primers are listed in Table S1.

2.6. Generation of VGLL3-expressing stable clones

VGLL3-expressing clones were generated by transfecting OV-90 cells with the commercially available pDream2.1 vector

containing the (sequence verified) *VGLL3* coding sequence in frame with the Flag tag sequence or empty pDream2.1 vector (GeneScript USA Inc., Piscataway, NJ, USA) using lipofectamine 2000 and Opti-MEM[®] (both from Life Technologies Inc., Burlington, ON, Canada). The *VGLL3*-expressing and empty vector clones were each selected and maintained in the presence of 800 µg/ml and 400 µg/ml of G418 (Wisent Inc.), respectively, in OSE complete medium.

2.7. Western blot analyses

Cells were lysed in RIPA buffer (Sigma–Aldrich, Oakville, Ontario, Canada) containing appropriate amounts of protease inhibitor cocktail (Roche Diagnostics, Laval, QC, Canada). Fifty µg of total protein were resolved by SDS-PAGE and transferred using iBlot[®] Gel Transfer Stacks (Life Technologies Inc.) onto a nitrocellulose membrane. The membranes were blocked with 5% milk and then incubated with the appropriate antibody (Table S2). Proteins were visualized using the ECL system (EMD Millipore, Billerica, MA, USA).

2.8. Lentivirus production and cell infection

The stable OV-90 clone expressing the tetracycline repressor (TetR), OV-90^{6/TR}, was generated by transfection of the pcDNA6/TR vector (Life Technologies Inc., cat. No. V1025-20) with Lipofectamine (Life Technologies Inc.) and maintained in OSE complete medium supplemented with blasticidin (Wisent Inc.) at 12 µg/ml. *VGLL3* inducible clones were generated by transfecting OV-90^{6/TR} with pLenti-CMV Puro that expresses the Flag-Tagged *VGLL3*, when grown in the presence of doxycycline (Enzo Life Sciences Inc., Farmingdale, NY, USA). The Gateway[®] Technology system (Life Technologies Inc.) was used to subclone the Flag-Tagged *VGLL3* coding sequence from pDream vector used in our transfection assays into a pDONR221 vector by a BP recombination followed by an LR recombination between pDONR221-*VGLL3*-Flag vector and the pLenti CMV/TO Puro DEST destination vector (670-1; Addgene #17293) (Campeau et al., 2009) and the construct was verified by sequencing. Lentiviruses were produced by co-transfecting the pLenti CMV/TO Puro DEST-*VGLL3*-Flag and the ViraPower Lentiviral Packaging Mix (Life Technologies Inc.) in the 293FT packaging cell line. The supernatant containing the viral particles was collected, concentrated by ultracentrifugation and then used to infect about 2×10^5 OV-90^{6/TR} cells per well of a 6-well plate containing 2 ml of culture medium with 5 µg/ml polybrene. Media was changed 16 h after infection and puromycin (Wisent Inc.) added after 48 h at 0.5 µg/ml. Infected OV-90^{6/TR} cells were induced by adding 20 ng/ml of doxycycline to the medium.

2.9. Immunocytochemistry

Cells were grown on coverslips in a 24-well culture plate for three days in complete OSE medium with or without 20 ng/ml of doxycycline, and then fixed in 1 ml of cold methanol (–20 °C) for 20 min. After three PBS washes cells were incubated with PBS containing 3% bovine serum albumin (Wisent Inc.) for an hour at room temperature. They were then stained with primary antibodies (Table S2) for 60 min in 3% PBS-BSA, washed, and incubated with secondary antibodies in 3%

PBS-BSA for 60 min (Table S2). The cell nuclei were stained with Hoeschst 33342 bis benzimide (Sigma–Aldrich). Mounted coverslips were analyzed under a Nikon Eclipse E600 microscope with objective lenses plan APO 20×: 20/0.6 NA (Nikon Canada, Mississauga, ON, Canada). Images were acquired with a cool snap HQ2 camera piloted by the NIS elements AR 3.0 acquisition software (Leica Camera Inc., Allendale, NJ, USA). Negative controls omitted the use of primary antibodies.

2.10. Tissue specimens

The HGSC and normal fallopian tube tissue samples were collected with informed written consent and granted approval from patients undergoing surgeries performed at the Centre hospitalier de l'Université de Montréal (CHUM) – Hôpital Notre-Dame. Clinical features such as disease stage, and tumor characteristics such as grade and histopathological subtype, were assigned by a gynecologic-oncologist and/or gynecologic-pathologist according to the criteria established by the International Federation of Gynecology and Obstetrics. Disease-free survival, defined according to the Response Evaluation Criteria in Solid Tumors (Therasse et al., 2000), as time to doubling of the upper normal limit of the serum cancer antigen marker CA-125 or the detection of a new lesion by ultrasound or CT-scan imaging, and overall survival, were extracted from the Système d'Archivage des Données en Oncologie. Written informed consent from all participants was in accordance with the Declaration of Helsinki and in compliance with the Research Ethics Boards of Centre hospitalier de l'Université de Montréal-Hôpital Notre-Dame and The McGill University Health Centre.

2.11. *VGLL3* expression analyses in normal tissues and HGSC samples

VGLL3 expression was assessed using a custom Ziplex[®] gene expression array (Axela, Inc. Toronto, ON, Canada) for 11 primary cultures of normal ovarian surface epithelial (NOSE) samples prepared as described previously (Quinn et al., 2009b), a commercially available RNA sample from a normal whole ovary sample (Agilent Technologies Canada Inc., Mississauga, ON, Canada) and 79 HGSCs. Details of array and probe design, and methodology have been described in detail (Quinn et al., 2009b). An independent sample t-test, not assuming equal variance, was performed to determine if *VGLL3* expression in the NOSE samples was significantly different from that of the HGSC samples using SPSS software (16.1) (Statistical Product and Service Solution Package, SPSS, 16.0, Chicago, IL, USA).

Immunohistochemistry (IHC) was performed on a tissue microarray (TMA), containing 0.6 mm tissue cores from 196 HGSCs and 11 normal fallopian tube samples from paraffin embedded tissue blocks selected based on a review of hematoxylin and eosin-stained slides (Wojnarowicz et al., 2012a). The cores were arrayed 1 mm apart onto a single paraffin block. IHC analysis was performed using 5 micron sections mounted onto frosted plus slides. Staining was performed with an antibody against human *VGLL3* (Table S2) using the Ventana Benchmark XT system (©Ventana Medical Systems, Inc., Tucson, AZ, USA). The TMA was scanned and the images were viewed using Olympus OlyVIA software 2.3 (Build 8529). Two observers examined the images independently and scored

both the epithelial ($n = 182$) and the stromal ($n = 180$) components of each core based on staining intensity and ranked it as negative, low or high. The inter-observer correlation coefficient was 0.785 for the epithelial component and 0.918 for the stromal component, and was calculated using SPSS software. The relationship between VGLL3 immunostaining (absent, low and/or high) and disease-free survival as defined above were evaluated using Kaplan–Meier survival curve analyses coupled to the Mantel–Cox log-rank test, and performed using SPSS software. *P*-values less than 0.05 were considered statistically significant.

2.12. Mutation analysis of VGLL3

Mutation analysis was performed by sequencing genomic DNA of the protein coding region and intron/exon splice junctions of HGSCs as previously described (Cody et al., 2009). The sequence variants were compared with those reported in the Single Nucleotide Polymorphism (dbSNP) database (www.ncbi.nlm.nih.gov/projects/SNP/). Variants resulting in amino acid substitutions were examined by PolyPhen (genetics.bwh.harvard.edu/pph/), Panther (www.pantherdb.org/tools/csnpscoreform.jsp), SNP effect (snpeffect.vib.be) and SIFT dbSNP (sift.jcvi.org/www/SIFT_dbSNP.html), and aligned to orthologous and homologous genes from various species using the UCSC Human Genome Browser Gateway hg19 assembly (genome.ucsc.edu) (Karolchik et al., 2003) in order to predict the possible impact on the structure and function of the encoded protein.

2.13. Electron microscopy

Cultures of OV-90, OV-90:VGLL3¹¹, OV-90:VGLL3²⁰, OV-90:EV, OV-90^{TR-VGLL3}, OV-90^{TR-ccDB} with or without doxycycline treatment, plated in eight-well Nunc Lab-Tek tissue culture chamber slides (Sigma–Aldrich), were grown to confluency and then washed in phosphate-buffered saline and fixed *in situ* with 3% glutaraldehyde in 0.1 M sodium cacodylate buffer (pH 7.4). After being washed several times with cacodylate buffer, the cell layers were treated with 1% osmium tetroxide in buffer, washed in buffer and then treated with 2% tannic acid in buffer, each for 30 min. Cell layers were then dehydrated in a graded series of ethanol to 70%, treated for 1 h with 2% uranyl acetate in 70% ethanol, and then washed in 70% ethanol. Cell layers were further dehydrated to 100% ethanol and then infiltrated with ethanol:Epon mixtures (1:1 and 1:3) and embedded in pure Epon (MECALAB, Ltd., Montreal, QC, Canada). En face thin sections (60 nm) were placed on formvar-coated grids and counterstained with 7% methanolic uranyl acetate followed by lead citrate. Sections were examined in a Tecnai 12 transmission electron microscope at an accelerating voltage of 120 kV, and images were digitally captured.

3. Results

3.1. Successful generation of OV-90 hybrids by MMCT of der3p12q12.1

To gather further evidence in support of a 3p12-pcen TSG, a functional gene complementation assay involving the

MMCT of der3p12-q11 chr into OV-90 was performed. The hybrids OVHA3-1, OVHA3-2, OVHA3-3 and OVHA3-4 were generated and stably maintained in cell culture, all lacking contaminating mouse chrs by FISH analyses (Figure S1). Genotype analyses using selected polymorphic microsatellite markers confirmed the presence of the transferred der3p12-pcen alleles (data not shown). A FISH analysis using a human chr 3 painting probe verified the presence of a small derivative chr 3 in all MMCT hybrids (Figure S1).

3.2. The MMCT hybrids exhibited different growth characteristics

The MMCT hybrids were compared with OV-90 for differences in cell morphology, and various *in vitro* and *in vivo* growth characteristics. All hybrids exhibited no overt differences in their cell morphology based on light microscopy (Figure 1A). In cell culture they propagated as a monolayer of tightly packed cells with a cobblestone-like appearance typified by epithelial cells, as demonstrated by OV-90 (Provencher et al., 2000). However, only OVHA3-1 exhibited a lower, but not significantly different, viability (data not shown) relative to OV-90 and the other hybrids, and has lost the capacity to form spheroids in hanging drop cultures (Figure 1B). Moreover, this hybrid as well as OVHA3-4 was unable to form colonies in soft agar, a feature suggesting that loss of anchorage independence of growth had occurred (Figure 1C). Although OV-90 and the hybrids were tumorigenic at s.c. and i.p. sites in a tumor xenograft mouse model (Figure 1D–F), OVHA3-1 tumor growth appeared to be significantly slower at s.c. sites ($p < 0.001$) (Figure 1D). Survival as measured by the time-to-sacrifice in both the s.c. and i.p. xenograft experiments was also significantly longer for OVHA3-1 ($p < 0.001$) (Figure 1E and F). At i.p. sites, the OV-90 derived tumors appeared vascularized and tumor formation was accompanied with bloody ascites. Although this was also the case with the tumors derived from OVHA3-2, OVHA3-3 and OVHA3-4, both the tumors and the accompanying ascites appeared noticeably less vascularized in experiments with OVHA3-1 (Figure 1F and S2).

3.3. Genetic analysis of the hybrids identified VGLL3 as TSG candidate

The MMCT hybrids were characterized for their chr 3p genetic content by a comparative analysis with OV-90 and the donor cell initially using polymorphic microsatellite markers, and then by genome-wide high-density SNP array analysis. Our genotyping results of the HA(3)IIaa donor hybrid cell line using polymorphic microsatellite markers suggested that the 3p centric fragment is defined by D3S2323 (3p12.3) and D3S1603 (3q12.1) consistent with independent findings (Sanchez et al., 1994; Zhang et al., 2007) (Figure 2A and S3). The combined analyses suggested that OVHA3-1 acquired and maintained the entire 3p interval of the derivative chr. This interval contains 10 known genes and only the first 2 exons of ROBO1 (Figure S4 and Table S3). In contrast, the other hybrids appeared to have acquired and/or maintained only a portion of the transferred chr. Hybrid OVHA3-3 appeared to have

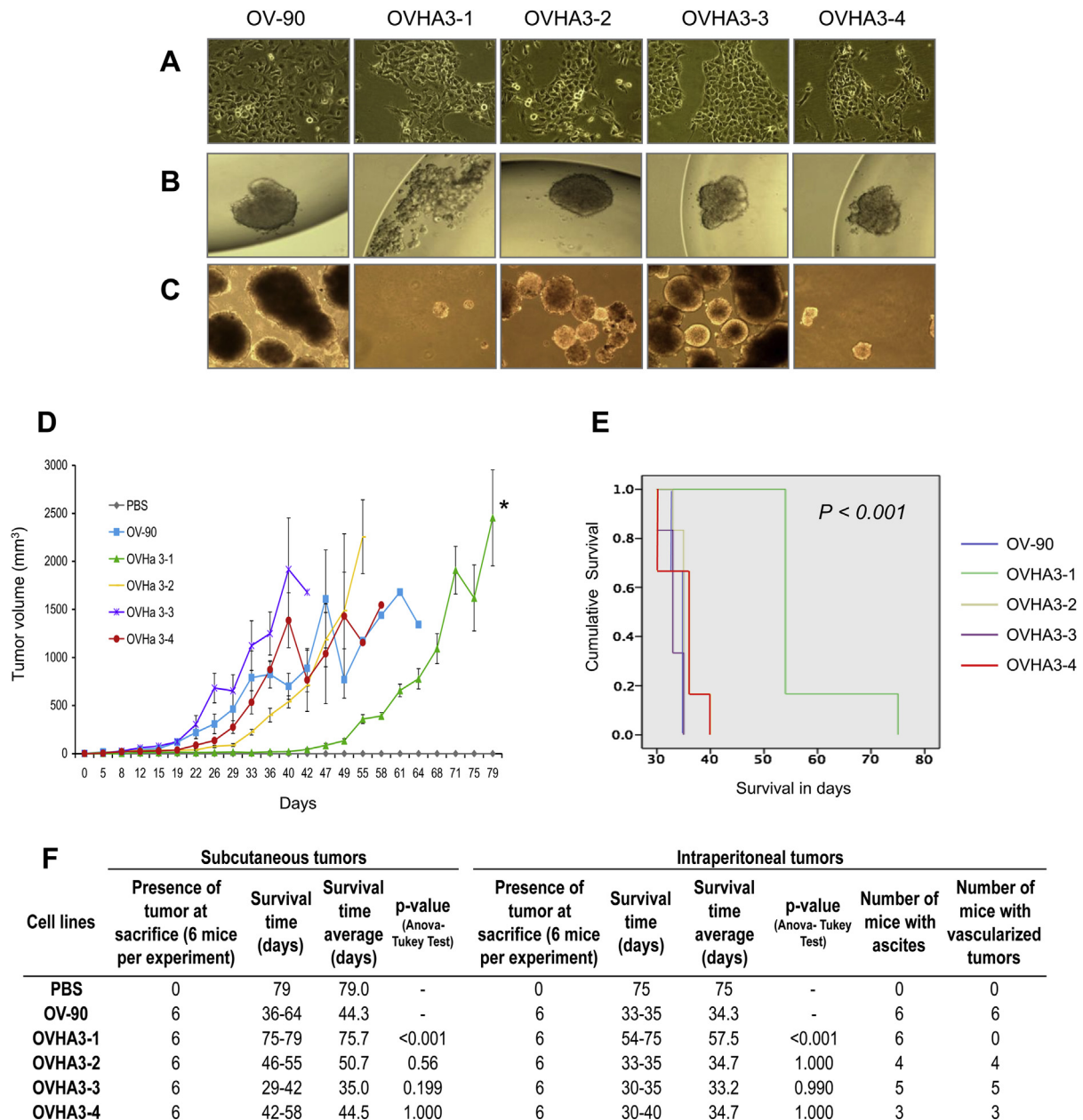


Figure 1 – Characterization of MMCT hybrids. (A) Morphological appearance of the OV-90 and MMCT hybrid cell lines, OVHA3-1, OVHA3-2, OVHA3-3 and OVHA3-4 ($\times 20$). (B) The capacity of the cells to form spheroids in hanging droplets was tested after 4 days ($\times 20$). (C) The colony forming ability of the cells in soft agar was monitored after 3 weeks ($\times 40$). (D) Tumor growth kinetics (mean of tumor sizes \pm SE) of OV-90 and the MMCT hybrids at subcutaneous (s.c.) injection site (to follow results of each group values were connected with lines) showing that OVHA3-1 tumor growth was significantly different than from OV-90 (*) (p -value < 0.05 , Mann–Withney U -test). (E) Kaplan–Maier survival curves for OV-90 and the MMCT hybrids at intraperitoneal (i.p.) injection site. (F) Data for s.c. and i.p. *in vivo* tumorigenicity assays of OV-90 and the four MMCT hybrids. Phosphate-buffer saline (PBS).

maintained a fragment containing the 3' end of *CHMP2B* (5 exons), *POU1F1*, *HTR1F*, *CGGBP1*, *ZNF654*, *C3orf38* and *EPHA3*, as well as a fragment containing the 5' end of *CADM2* but excluding exons 6 to 10. Although the hybrid OVHA3-3 also maintained two other fragments, neither is known to contain an intact gene. The hybrid OVHA3-4 maintained a fragment containing only *GBE1*. It was difficult to properly assess the content of transferred genes in OVHA3-2, as this hybrid exhibited evidence of genomic instability and loss of

transferred alleles (Figure 2A and S3). A comparative genetic analysis of hybrids suggested that, only OVHA3-1 had uniquely acquired apparently uninterrupted *CADM2*, *VGLL3* and *CHMP2B* loci as a consequence of MMCT (Figure 2B, C and Table S3). As OVHA3-1 was the only hybrid exhibiting evidence of altered tumorigenic potential (Figure 1), it is possible that the introduction and expression of these genes contributed to the tumor suppressor phenotype exhibited by this hybrid.

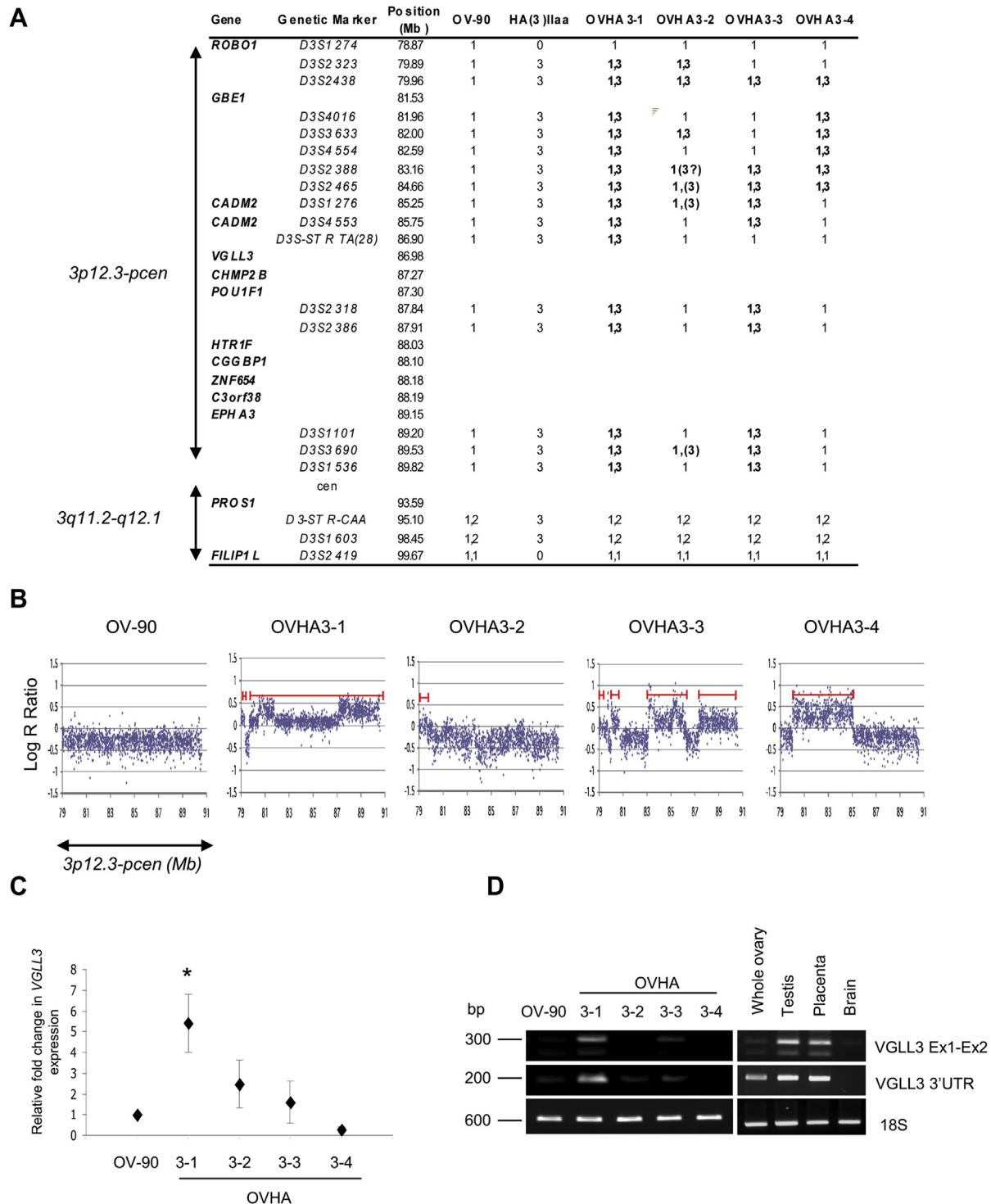


Figure 2 – Genetic analyses of the 3p12-q12 region in the MMCT hybrids. (A) Genotypes of the MMCT hybrids, parental OV-90 cell line and HA(3)IIaa 3p12-q12 donor cell line based on polymorphic microsatellite markers analyses. The data is aligned according to genomic position based on Human Genome Browser Gateway hg19 assembly where distance megabases (Mb) is relative to 3p-telomere. Alleles (1,2) derived from the OV-90 were distinguished from the HA(3)IIaa allele (3). Alleles exhibiting imbalance are in brackets. (B) Genotyping data from SNP BeadArray analyses of OV-90 and the MMCT hybrids showing copy number (highlighted with red line) represented as Log *R* Ratio using the BeadStudio Data Analysis software of 3p12.3-pcen interval aligned to chromosomal position (Mb, x-axis). (C) Quantitative real time PCR analysis of *VGLL3* in the MMCT hybrids (OVHA-1, OVHA-2, OVHA-3, and OVHA-4) normalized to expression values (\pm SE of four experiments performed in duplicate; significant differences ($*p < 0.05$) evaluated by *t*-test) observed in OV-90 parental cell line. (D) Semi-quantitative RT-PCR analysis of *VGLL3* in OV-90 and 4 MMCT (OVHA-1, OVHA-2, OVHA-3, and OVHA-4) hybrids using oligonucleotide primers that amplified either a portion of 3'UTR or message spanning exons 1 and 2 of *VGLL3*, where the expression of *18S* is shown as a control for RNA quality. PCR products are shown relative to size markers (in basepairs (Bp)).

3.4. Loss of *der3p12-pcen* donor alleles in the OVHA3-1 xenografts

We investigated the genetic content of the xenografts derived from OVHA3-1 to determine if the transferred alleles were retained in the tumors. Whole genome genotyping analyses were performed on independently derived tumor samples, XT1 and XT2, from s.c. sites and compared to that of hybrid OVHA3-1, which was maintained under G418 selection in tissue culture (to select for cells harboring the *der(3) neo^r* tagged chr) and genotyped prior to performing the *in vivo* tumorigenicity assays (Figure S5A). The genotyping results suggested that loss of the introduced fragment had occurred in a subpopulation among the tumor cells. To explore this notion further, XT1 cells were assayed for sensitivity to G418 and assays demonstrated loss of 50% of cells in culture when grown in the presence of G418 (Figure S5B). The cells from five independently derived tumor xenografts from s.c. sites were also assayed for their ability to form spheroids in hanging drop culture, as this feature was altered in OVHA3-1 (Figure 1). The capacity to form spheroids in the presence of G418 appeared unchanged (Figure S5C). However, in the absence of G418, the cells from OVHA3-1 derived tumor xenografts formed a number of small aggregates rather than large defined spheroids. All of these results raise the possibility that the delay in tumor formation could have been due to the selection of hybrid cells that have lost the introduced alleles.

3.5. VGLL3 expression in MMCT hybrids

The comparative genetic analysis and tumorigenicity experiments involving the MMCT hybrids suggested that the *CADM2*, *VGLL3* and *CHMP2B* loci as potential candidates to pursue as tumor suppressors. These findings are consistent with our previous chromosome 3 fragment transfer experiments involving OV-90 cell line which also showed loss of tumorigenic potential in the hybrids that had acquired these loci (Cody et al., 2007). However, we pursued *VGLL3* as the primary candidate as our previous comparative gene expression analyses of *CADM2* and *CHMP2B*, which is contiguous with *VGLL3* do not support a role for these genes as tumor suppressors in ovarian cancers (Cody et al., 2009).

VGLL3 expression was investigated in the MMCT hybrids using qRT-PCR in order to confirm that the introduced alleles were transcriptionally active as have been observed in our previous analyses of chromosome 3 transfer experiments (Cody et al., 2007, 2009). OVHA3-1 exhibited the highest level of expression of *VGLL3* relative to OV-90, and this was significantly different as compared with OV-90 and the other hybrids (Figure 2C). RT-PCR analyses also indicated low level of *VGLL3* expression in OVHA3-3. Moreover, differential RT-PCR analyses showed two distinct bands associated with *VGLL3* amplification that we have attributed to the expression of a full-length transcript and an alternative shorter length transcript in OVHA3-1 (Figure 2D). The alternative size transcript is consistent in size with our previous *VGLL3* expression analyses in chromosome 3 transfer OV-90 derived hybrids, ovarian cancer specimens (at low levels) and normal tissues, and has

been verified by DNA sequencing (Cody et al., 2009). The function of the alternative transcript is unknown, however relative to the full-length sequence, it harbors in-frame deletion of 159 nucleotides that is predicted to result in an absence of 59 amino acids overlapping the putative TEAD1 interaction domain in the encoded protein (Cody et al., 2009).

3.6. Generation of VGLL3 expressing OV-90 derived transfectant clones

To assess the biological effect of highly expressing *VGLL3* in OV-90, we used a commercially available construct, where *VGLL3* expression was controlled by the CMV promoter and the encoded protein detectable by an anti-Flag antibody. We used this construct as attempts at generating stable *VGLL3* expressing OV-90 clones using a pcDNA3 expression vector were unsuccessful though transient transfection assays demonstrated robust *VGLL3* expression had occurred as referred to in our previous study (Cody et al., 2009). About 50% (27 of 50) of clones were successfully maintained as clonal expansions in tissue culture, as compared with the 16 empty vector derived clones where all were maintained in culture. The *VGLL3*-expressing clones exhibited variable expression as compared with OV-90, OVHA3-1 and the transiently transfected OV-90 cells, with 21 of 27 clones exhibiting at least a 2-fold level of *VGLL3* expression by qRT-PCR analyses (Figure 3A). The OV-90:*VGLL3*¹¹ and OV-90:*VGLL3*²⁰ clones were selected for further analysis as they exhibited the highest levels of *VGLL3* expression (Figure 3B). Two empty vector clones were randomly selected for comparative analyses. Notable is that *VGLL3* expression by RT-PCR was significantly less detectable (relative to qRT-PCR analysis) for the *VGLL3*-expressing clones as compared with the transiently transfected OV-90 cells (Figure 3C). Western blot analysis using an anti-Flag antibody detected variable but noticeably lower levels of encoded *VGLL3*-Flag protein in OV-90:*VGLL3*¹¹ and OV-90:*VGLL3*²⁰ and other selected *VGLL3* transfectant clones compared with transiently transfected cells (Figure 3D). These findings combined with our previous attempt using pcDNA3, suggest that deriving stable transfectant clones expressing high levels of *VGLL3* in OV-90 cells may be difficult to achieve.

3.7. The VGLL3 expressing OV-90 clones exhibited a unique intracellular morphology

In contrast to OV-90, the *VGLL3*-expressing transfectant clones exhibited a distinctive intra-cellular morphology typified by the presence of numerous vacuole-like structures in the cytoplasm that were clearly visible by light microscopy (Figure 3E). These vacuoles did not appear to stain intensely with Oil Red O by visual assessment beyond background levels, indicating that they did not contain a significant lipid content as compared with control cells known to express a high lipid content (Figure S6). As these vacuoles have been reported in the context of autophagy (Codogno et al., 2011), we investigated by western blot analysis, the accumulation of the microtubules associated protein light chains LC3-II relative to LC3-I which has been described as a marker of autophagy (Kabeya et al., 2004). There appeared to be no visible difference in LC3-II relative to LC3-I levels in the *VGLL3*

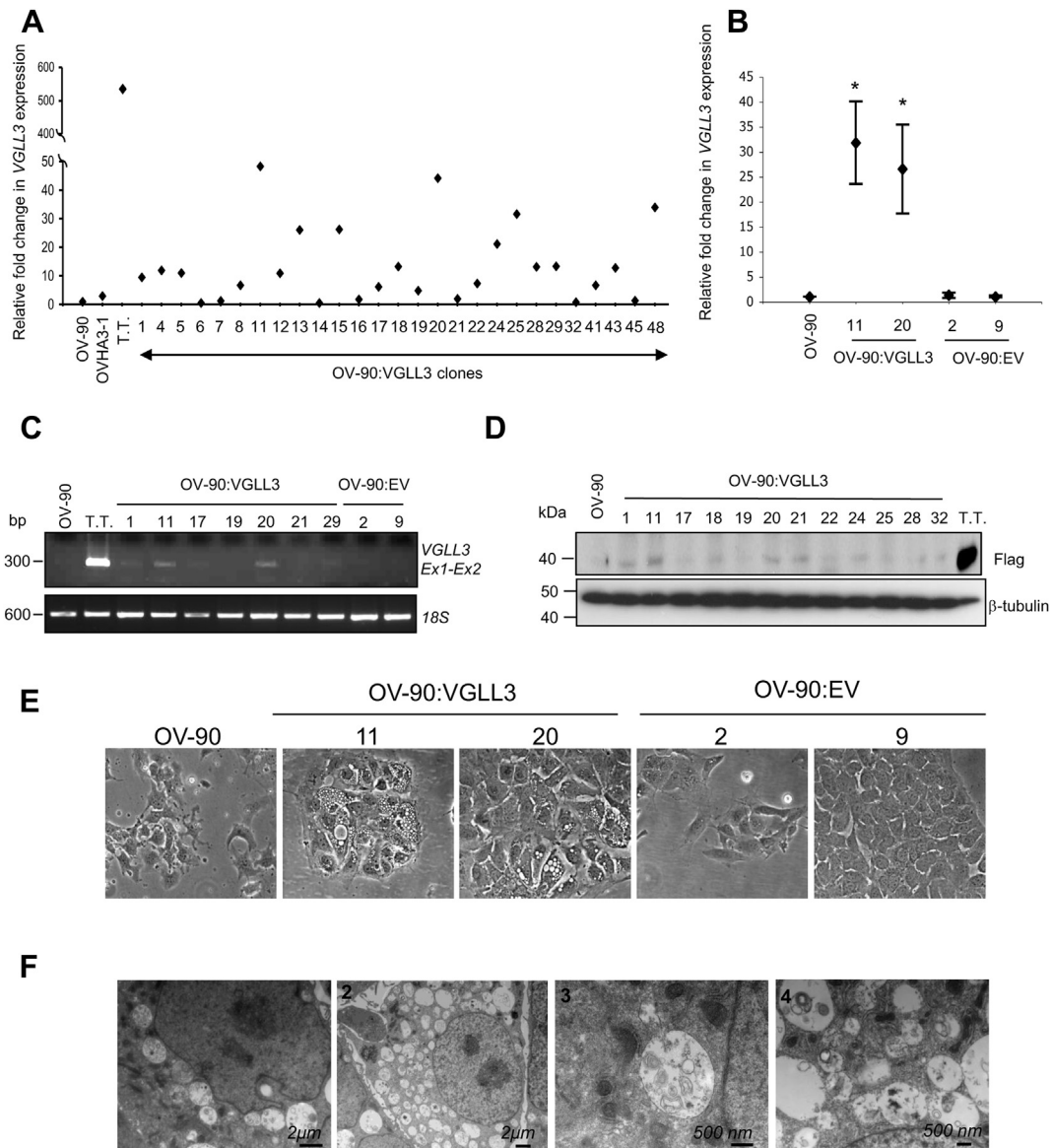


Figure 3 – Generation of stable *VGLL3*-expressing clones and cell morphology. (A) *VGLL3* expression levels based on quantitative real time PCR analysis of OV-90:VGLL3 clones (numbered), MMCT hybrid OVHA3-1, transiently transfected OV-90 cells (T.T.) relative to OV-90 cell line. (B) *VGLL3* expression levels (mean of three independent experiments) based on quantitative real time PCR analysis of OV-90:VGLL3¹¹, OV-90:VGLL3²⁰, OV-90:EV² and OV-90:EV⁹ relative to OV-90 cell line (significant differences ($*p < 0.05$) evaluated by *t*-test). (C) Semi-quantitative RT-PCR analysis of *VGLL3* in OV-90:VGLL3 and OV-90:EV stable clones where expression of *18S* is shown as a control for RNA quality. PCR products are shown relative to size markers (in basepairs (Bp)). (D) Western blot analysis of OV-90, OV-90:VGLL3 stable clones and OV-90 transiently transfected cells (T.T) using an anti-Flag antibody. β -tubulin was used as loading control. (E) Light microscope ($\times 40$) photographs of OV-90, OV-90:VGLL3¹¹, OV-90:VGLL3²⁰, OV-90:EV² and OV-90:EV⁹ cells showing cytoplasmic vacuoles in the *VGLL3*-expressing clones: OV-90:VGLL3¹¹ and OV-90:VGLL3²⁰. (F) Electronic microscopy images of OV-90:VGLL3¹¹.

expressing clones as compared with assays of OV-90 and the empty vector clones (Figure S7A). Electron microscopy was performed to characterize the vacuole-like structures, as cytoplasmic autophagic vacuoles result from the sequestration of cytosol or cytoplasmic organelles and thus have a double membrane (Codogno et al., 2011). The majority of the vacuoles lacked the characteristic double membrane typified by autophagic vacuoles, although there were many examples where they contained membranous structures (Figure 3F). These structures appear to be unique to the *VGLL3* expressing

transfectant clones as they were not visible in our MMCT derived hybrids nor our previously derived chr 3 fragment transfer hybrids (Cody et al., 2007).

3.8. The *VGLL3* expressing OV-90 clones exhibited modest alterations in growth phenotypes

To further assess the biological effect of expressing *VGLL3* in OV-90, we investigated several of the *in vitro* growth characteristics that were shown altered in the MMCT hybrids. The cell

viability appeared unchanged between the different clones and the parental OV-90 cell line (data not shown). We then assessed the spheroid formation capacity for each clone and compared results with two randomly selected empty vector derived transfectant clones. Interestingly, both the *VGLL3*-expressing clones and the empty vector clones had lost their ability to fully form spheroids with defined margins in hanging drop assays (Figure 4A). However, the empty vector clones formed larger multicellular aggregates (particularly OV-90:EV²) than those observed with the *VGLL3*-expressing clones. We were puzzled by these observations and performed spheroid formation assays on additional empty clones ($n = 5$), which yielded similar results (data not shown). While control empty vector clones still formed large multicellular aggregates instead of spheroids with defined margins as observed with OV-90, this capacity to do so was completely lost in the *VGLL3*-expressing clones.

The *VGLL3*-expressing clones were also compared with the empty-vector clones in clonogenic assays. There were no significant differences in the number of colonies formed in this assay between the different clones. However, it is interesting to observe that the *VGLL3*-expressing clones gave rise to colonies that were significantly smaller in size when compared with the empty vector clones (Figure 4B and C).

To assess whether *VGLL3* expression in OV-90 cell line background would affect tumor forming capacity, we performed *in vivo* tumorigenic assays at both s.c. and i.p. sites using a xenograft mouse model. The capacity to form tumors was not significantly different when the *VGLL3* expressing transfectant clones were compared with the empty vector clones at s.c. sites (Figure 4D and F). At i.p. injection site, there was no significant difference in survival time between the *VGLL3*-expressing group and the empty vector control group. Notable was that both of these groups were significantly different when compared with OV-90 parental cell line at i.p. injection sites (Figure 4E). While we attribute these differences to selection of clones, our comparative analyses of transfectant clones derived from OV-90 do not support the notion that expressing *VGLL3* in OV-90 cell affected tumorigenic potential.

As our previous MMCT assays showed loss of the transferred 3p fragment in the resulting xenograft tumors, we examined the *VGLL3* expression in the xenograft tumors derived from the *VGLL3*-expressing clones. Interestingly, *VGLL3* expression was no longer detectable in any of the OV-90:VGLL3¹¹ and OV-90:VGLL3²⁰ tumor xenografts (derived at both s.c. or i.p. sites) tested by RT-PCR (Figure S8). These results strongly support the notion that deregulation or silencing of *VGLL3*-expression in OV-90 transfectant clones was required for tumor formation.

3.9. Lentivirus inducible *VGLL3*-expressing OV-90 cells also exhibited unique intracellular morphology

We turned to a lentivirus inducible system to try to induce higher levels of *VGLL3* expression in OV-90, as all of our stable clones expressed *VGLL3* at modest levels despite the use of a vector construct with the strong CMV promoter. First, OV-90^{6/TR} clones were derived from the transfection of pcDNA6/TR, a vector that expressed the tetracycline repressor (TetR). A OV-90^{6/TR} clone was then transfected with pLenti-CMV Puro (OV-90^{6/TR} ccDB, used as negative control) or pLenti-

CMV Puro-*VGLL3* vector that expresses Flag-tagged *VGLL3* (OV-90^{6/TR-VGLL3}) when such cells were grown in the presence of doxycycline. RT-PCR analysis showed that OV-90^{6/TR-VGLL3} transfected cells exhibited noticeably higher levels of *VGLL3* expression even in absence of doxycycline (Figure 5A). However, *VGLL3* protein expression was noticeably different in induced cells by both western blot and immunocytochemistry analyses using both anti-Flag and anti-*VGLL3* antibodies, which became available during the course of this study (Figure 5B and C). The induction of *VGLL3* expression did not appear to have overtly affected cell survival (data not shown). However, OV-90^{6/TR-VGLL3} induced to express *VGLL3* contained a larger proportion of cells with numerous intracellular vacuoles (Figure 5C) reminiscent of the morphological features observed with the *VGLL3*-expressing transfectant clones (Figure 3E). Electron microscopy also revealed cytoplasmic structures similar to those found in the *VGLL3*-expressing transfectant clones (data not shown). The paucity of vacuoles with double membranes combined with insignificant differences in the LC3-II:LC3-I levels suggested that autophagy was also unlikely induced in these cells (Figure S7B). Moreover, OV-90^{6/TR-VGLL3} induction of *VGLL3* expression did not exhibit increased apoptotic activity as measured by cleavage of caspase-3 by immunoblot assay (data not shown).

3.10. *VGLL3* protein expression and cell localization

Until recently, studies of *VGLL3* protein expression were hampered by the lack of a specific *VGLL3* antibody, and our attempts to have an antibody commercially synthesized were not successful (data not shown). As mentioned above, a commercial polyclonal rabbit anti-*VGLL3* antibody, ab83555, became available during the course of our study. Initial western blot analyses revealed low levels of reactivity of OV-90:VGLL3 expressing transfectant clones as compared with OV-90 (data not shown), possibly due to the low expression levels of *VGLL3* expression as inferred by RT-PCR analysis or western blot analysis using an anti-Flag antibody (see Figure 3C and D). However, the new *VGLL3*-antibody appears to detect a *VGLL3* Flag-tagged protein of predicted size as indicated by western blot analysis of doxycycline induced OV-90^{6/TR-VGLL3} cells (Figure 5B). Immunofluorescence images of doxycycline exposed OV-90^{6/TR-VGLL3} cells exhibited clear evidence of immunoreactivity with anti-*VGLL3* antibody, as compared to the control cells regardless of exposure to the inducer. The modest immunoreactivity observed in the OV-90^{6/TR-VGLL3} cells grown in the absence of the inducer, is consistent with the 'leaky' phenotype of this construct (Figure 5A and C). Immunocytochemistry (ICC) suggests both a nuclear and perinuclear localization of *VGLL3* protein in overexpressing cells (Figure 5C and S9), which is consistent with its purported function as a transcription co-factor (Maeda et al., 2002).

3.11. *VGLL3* gene and protein was underexpressed in HGSCs and this was not attributed to somatic intragenic mutations

Previous gene expression analyses suggested low levels of *VGLL3* expression in a limited set of HGSCs relative to NOSE (Cody et al., 2009). Using a custom-made gene expression

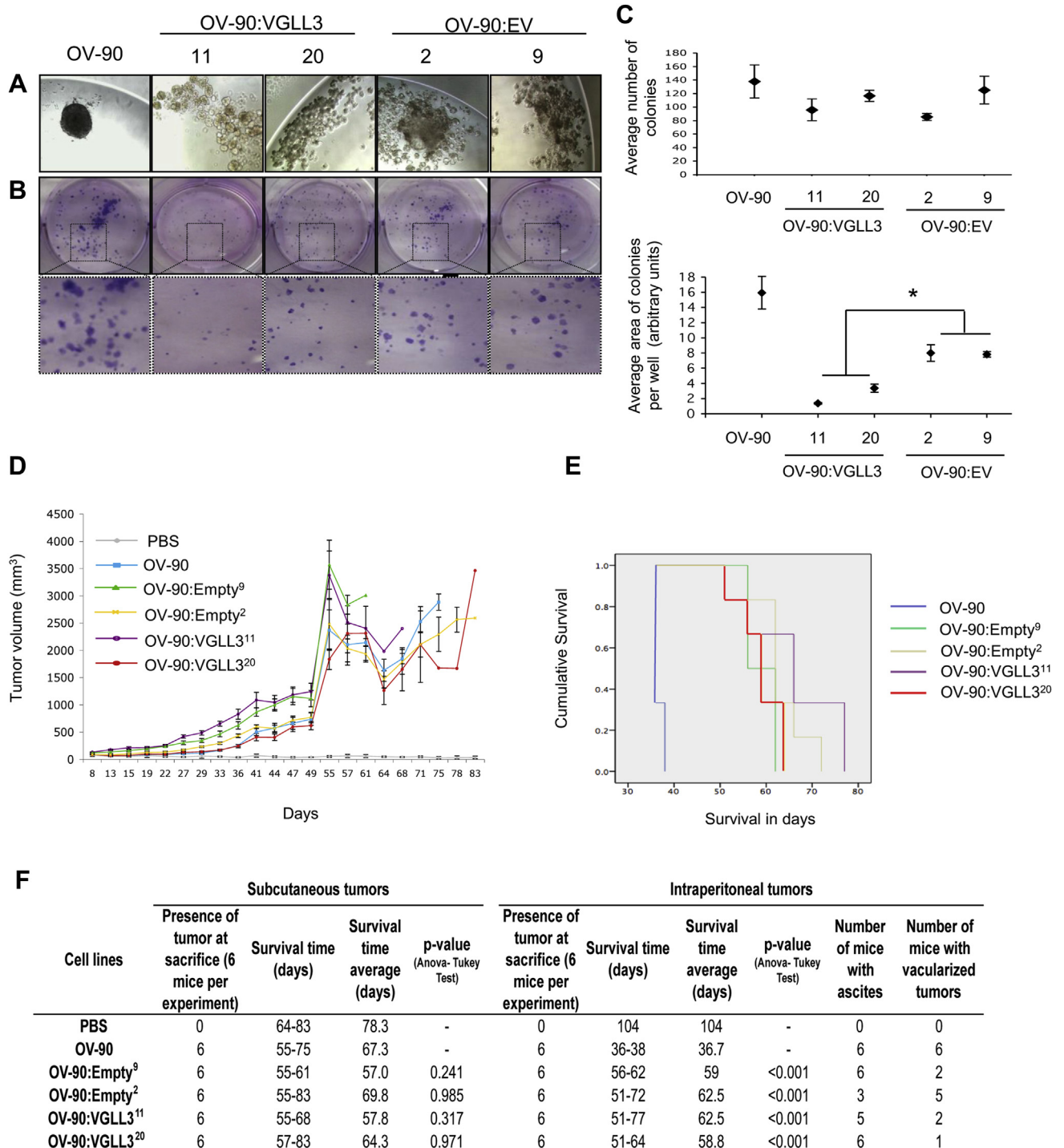


Figure 4 – Characterization of the VGLL3-stable clones. (A) Light microscopy images (×20) of cells in hanging drop cultures for spheroid formation assays of OV-90, and the OV-90:VGLL3 and OV-90:EV stable clones. (B) Images of results from clonogenic assays (1× and 4×). (C) Average number of colonies (values represent the mean ± SE of number of colonies for each group in four experiments) and the total surface area of the colonies (values represent the mean ± SE of the total colony area per well for each group of three independent experiments) formed in clonogenic assays. (D) Tumor growth kinetics of OV-90, OV-90:VGLL3¹¹, OV-90:VGLL3²⁰, OV-90:EV² and OV-90:EV⁹ at subcutaneous injection (s.c.) site in mouse tumor xenograft assays. The mean of tumor sizes ± SE is reported on the graph for each group. Mann–Withney *U*-test indicates no significant difference in the tumor growth kinetics. (E) Kaplan-Meier survival curves of OV-90, OV-90:VGLL3¹¹, OV-90:VGLL3²⁰, OV-90:EV² and OV-90:EV⁹ at i.p. injection site. A *post hoc* Tukey test indicated a significant difference with a *p*-value < 0.001 in the survival time between OV-90 and each of OV-90:VGLL3¹¹, OV-90:VGLL3²⁰, OV-90:EV² and OV-90:EV⁹ at i.p. injection sites, but no significant difference between OV-90:VGLL3¹¹ and OV-90:VGLL3²⁰ with OV-90:EV² and OV-90:EV⁹. Information related to survival time range and average of mice, the presence of tumors, ascites and evidence of vascularization are reported (F).

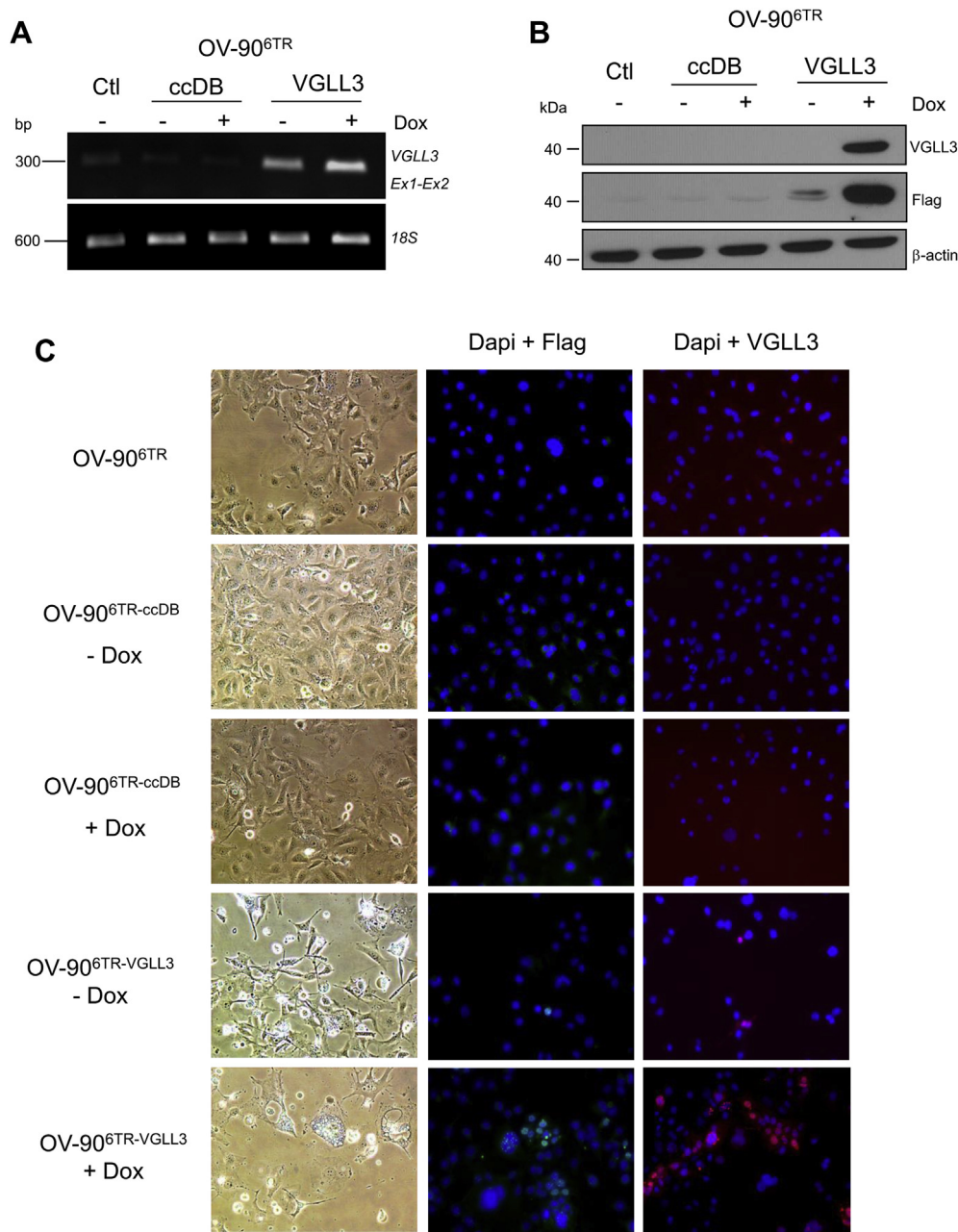


Figure 5 – VGLL3 gene and protein expression in OV-90, OV-90^{6TR-VGLL3} and OV-90^{6TR-ccDB} inducible clones. (A) Semi-quantitative RT-PCR analysis of VGLL3 in the absence (–) or presence (+) (3 days) of doxycycline (Dox). (B) Western blot analysis of protein extracted from cells in the absence (–) or presence (+) (3 days) of doxycycline detected using anti-Flag and anti-VGLL3 antibodies. (C) Cell morphology of OV-90, OV-90^{6TR-VGLL3} and OV-90^{6TR-ccDB} inducible clones without (–) or with (+) (10 days) doxycycline. VGLL3 expression resulted in cells with cytoplasmic vacuoles and a more elongated cell shape. Immunofluorescence detection of VGLL3 without (–) or in presence (+) (3 days) of doxycycline detected using anti-Flag, or anti-VGLL3 antibodies.

array platform (Quinn et al., 2009b), we have extended the sample set to include 79 TP53 mutation-positive HGSCs (Wojnarowicz et al., 2012b). About 76% HGSCs exhibited expression levels lower than that observed in whole ovary (Figure 6A). Relative to the mean of expression in the NOSE samples, VGLL3 was significantly underexpressed in 99% of HGSCs ($p = 0.007$) (Figure 6A).

We also investigated protein expression by IHC of a TMA that contained 196 HGSCs that included cores from 61 HGSCs

examined by gene expression. The vast majority (98.9%) of the epithelial tumor cell components of the HGSCs exhibited either no or low levels of staining (Figure 6C). There were no significant differences in the relationship between the overall or disease-free survival time of HGSCs with the intensity levels of VGLL3 immunostaining in both the epithelial and the stromal component of the core (Figure 6D), though there appeared to be more cases with evidence of higher staining levels in stromal tissue component from HGSC cases that had

a prolonged disease-free survival ($p = 0.08$). The majority (90.5%) of the stromal components of the tumor also exhibited no or low staining levels (Figure 6C). Although no cores were available from whole ovary with intact NOSE, the tissue array contained cores containing normal fallopian tube samples, which is a recently posited origin of some HGSCs (Salvador et al., 2009). Notable was that VGLL3 staining was also evident in the fallopian tube epithelial (FTE) cells (Figure 6B).

To determine if VGLL3 expression was associated with an intragenic alteration, we sequenced the protein encoding regions and splice sites of VGLL3 in the HGSCs that were investigated by both gene and protein expression. With the exception of c.578 A > T variant found in exon 3 in one sample no other variants were identified. This variant, reported in the dbSNP Database as rs79345443, is predicted to confer an amino acid substitution of His (CAT) for Leu (CTT) at position 193 in VGLL3, and has been found in 3.5% of the European population tested ($2n = 1324$ chromosomes) [http://www.ncbi.nlm.nih.gov/SNP/snp_ss.cgi?ss=ss491837946]. The consequences of this alteration are unknown, however the His193Leu variant and immediately flanking amino acids appear to reside in a highly conserved region among primates as determined by Vertebrate Multiz Alignment and Conservation analysis of 46 species (genome.ucsc.edu). The computational tools PolyPhen, Panther and SIFT dbSNP predicted that this substitution had a functional effect, whereas SNP effect did not. The variant was also found in the germline DNA of this same patient. Notable is that our previous genetic analysis of OV-90 also did not identify any evidence for somatic inactivation of VGLL3 (Cody et al., 2009). These results suggest that an alternative mechanism accounts for deregulating VGLL3 expression in HGSC.

4. Discussion and conclusions

Our microcell mediated chromosome 3p12-q12 transfer experiments have provided further support for the notion that this genomic region contains at least one gene that confers a tumor suppressor phenotype. Our previous molecular genetic analyses of genes in 3p12 interval suggested that VGLL3 was a strong candidate to pursue (Cody et al., 2007,2009). This is further supported by the observation that only OVHA3-1 MMCT hybrid that had acquired the der3p12-pcen chr containing the VGLL3 locus, exhibited alterations in both *in vitro* growth characteristics and *in vivo* tumorigenic potential in a mouse tumor xenograft model, where a delay in tumor formation was observed. These findings differ in part from our previous studies in that OV-90 hybrids generated by chr 3 fragment transfer experiments exhibited complete suppression of tumorigenicity (Cody et al., 2007). The failure of MMCT hybrid cells that retained der3p12-pcen to thrive *in vivo* could have accounted for our observations, as suggested by the loss of transferred alleles in OVHA3-1 derived xenografts.

Our inability to derive stable OV-90 transfectant clones that highly express VGLL3 is intriguing. Only stable low-level VGLL3-expressing clones were derived despite the use of a vector with a strong CMV promoter. Though there were visible differences in the capacity to form spheroids in hanging

drop cultures or colonies in clonogenic assays, the VGLL3-expressing and the empty vector clones did not significantly differ in tumorigenic potential in mouse xenograft models. Notable however, is that loss of VGLL3 expression was observed in tumors derived from mouse xenografts. Though there was no delay in tumor formation *in vivo* as was observed with OVHA3-1, these results strongly suggest that deregulation or silencing of VGLL3-expression in OV-90 transfectant clones was required for tumor formation. The context wherein which VGLL3 expression occurs in cDNA expressing clones and from a derivative chromosome 3 in OVHA3-1 could explain these differences in tumorigenic potential, where the latter could be subject to cis-regulatory elements as well as the possibility that other genes co-transferred may have contributed to the phenotype as discussed further below. While our cell transfectant experiments may be equivocal, they raise the possibility that expression of VGLL3 in OV-90 cells, even at the modest levels observed in the stable transfectant clones, is incompatible with tumor formation.

Another interesting observation is that the VGLL3-expressing clones exhibited an unexpected intracellular phenotype consistent with MVB. The vacuoles in our clones are reminiscent of MVB as has been described in the context of the Endosomal Sorting Complex Required for Transport (ESCRT) pathway (Henne et al., 2011; Katzmman et al., 2002). We have attributed MVB formation to VGLL3 expression in this experimental context, as this phenotype was not observed in the empty vector clones but was also observed in the context of VGLL3 expression induced in the lentiviral system. MVBs were not observed in our MMCT assays or previous experiments involving chromosome 3 fragment transfer in OV-90. It is possible that expression derived from the protein encoding sequences representing only the full-length transcript from a strong CMV promoter may have contributed to this phenotype in this context. Though speculative, overexpression of a putative transcription factor, which is the purported function of VGLL3 based on the presence of a sequence with similarity to a TEAD1 transcription enhancer factor interaction domain protein motif (Legent et al., 2006; Maeda et al., 2002; Vaudin et al., 1999), may have strongly invoked the expression of genes whereby the consequences were observed inducing the ESCRT pathway. Moreover, VGLL3 expression from the introduced derivative chromosome 3p12.3-q12 would include cis-regulatory elements, which may have affected expression in this context. This includes an unusually long 10 kb 3'UTR of unknown function. Interestingly, RT-PCR analysis of VGLL3 expression also indicated that the expression of alternative smaller transcript occurred in the OVHA3.1 hybrid. The alternative size transcript is consistent in size with our previous VGLL3 expression analyses in chromosome 3 transfer OV-90 derived hybrids, ovarian cancer specimens (both at low levels when detected) and normal tissues, and has been verified by DNA sequencing (Cody et al., 2009). Relative to the full-length transcript, it harbors in-frame deletion of 159 nucleotides that is predicted to result in an absence of 59 amino acids overlapping the putative TEAD1 interaction domain in the encoded protein (Cody et al., 2009). The role of this alternative transcript is unknown, however, it was not detected in the RT-PCR analysis of the VGLL3 expressing transfectant clones. Further studies are

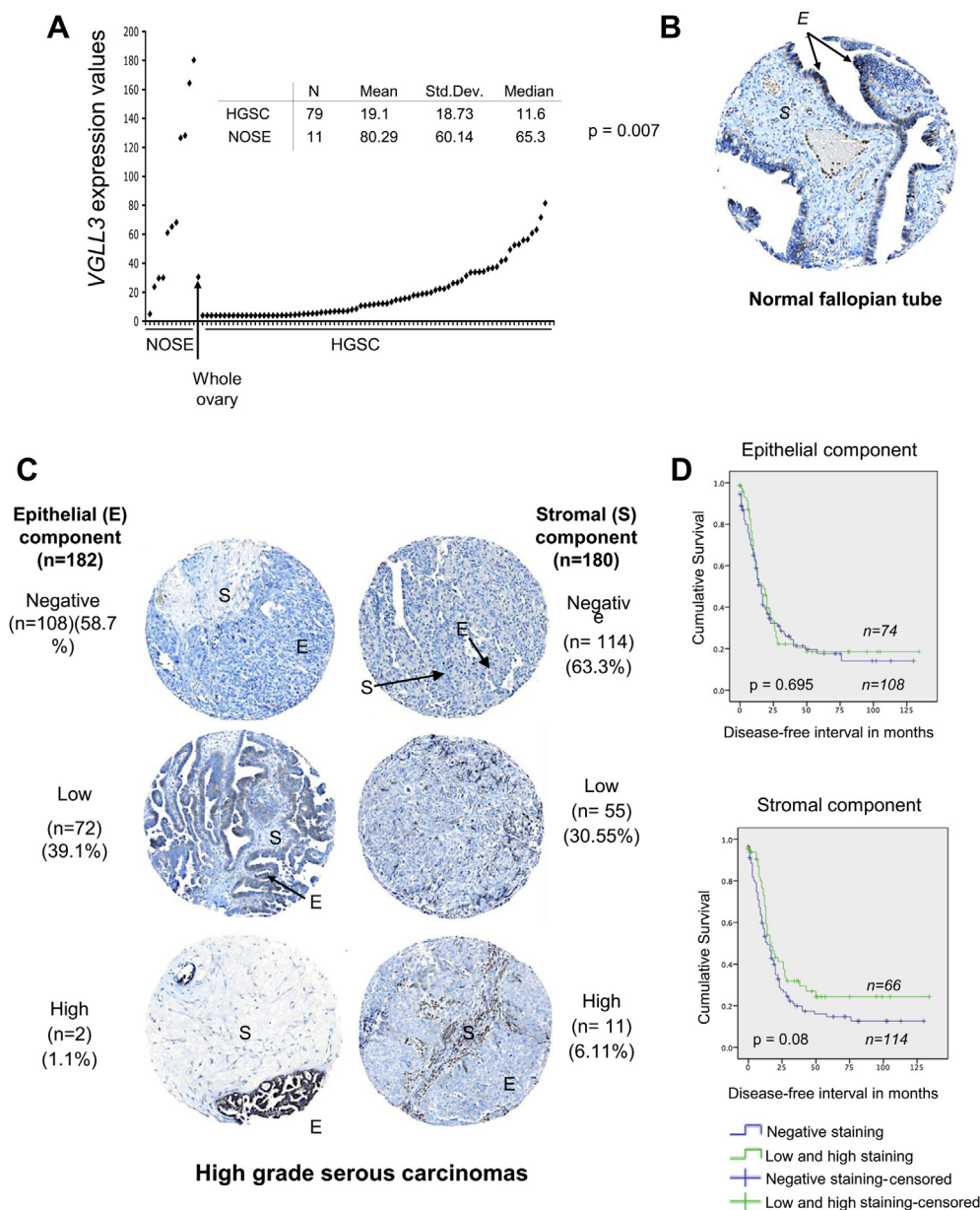


Figure 6 – VGLL3 gene and protein expression in high grade serous ovarian carcinomas (HGSC). (A) *VGLL3* expression in NOSE samples ($n = 11$), normal whole ovary and HGSC samples ($n = 79$) as assayed by Zplex Research System expression array. **(B)** An example of immunohistochemistry analysis of VGLL3 protein using anti-VGLL3 antibody of a paraffin embedded normal fallopian tube tissue core from a tissue microarray. **(C)** Examples of different staining patterns of immunohistochemistry analysis of VGLL3 protein using anti-VGLL3 antibody of a paraffin embedded HGSC tumor (epithelial (E) or stromal (S) components) tissue core from tissue microarray. **(D)** Kaplan–Meier survival curve analysis of HGSC cases for disease-free survival (in months) of patients whose tumors showed negative staining (blue curve) compared with patients whose tumors showed low or high staining (green curve) for VGLL3 protein in the epithelial or stromal components of the tumor (p -values were derived from log-rank tests).

warranted to investigate the role of alternative transcripts and other potential cis-acting genetic elements regulation of *VGLL3* expression.

We have demonstrated that *VGLL3* gene and protein expression was low or absent in the majority HGSCs. Our gene expression results are consistent with various global gene expression profiling studies of ovarian cancer specimens that include HGSCs as compared with either NOSE or FTE where different gene expression platforms were applied

(Anglesio et al., 2008; Birch et al., 2008; Bonome et al., 2005; Bowen et al., 2009; Cody et al., 2007; Jiang et al., 2010; Pejovic et al., 1992; TCGA, 2011; Tung et al., 2009) (see Table S4). Our gene expression results are consistent with our immunohistochemistry expression assays of HGSCs. These results, together with the gene expression observed in NOSE and protein expression observed in FTE, which are both the purported cells of origin for HGSC (Auersperg et al., 2001; Salvador et al., 2009), suggest the intriguing possibility that

VGLL3 expression is repressed in this cancer. The near ubiquitous suppression of VGLL3 may be important in the disease development as has been proposed in regards to the near ubiquitous presence of TP53 mutations in HGSCs (Singer et al., 2005). The consistent absence or low level of VGLL3 expression in clinical specimens relative to normal tissue is compatible with the notion that VGLL3 is involved in tumor suppressor pathways.

Genetic mechanisms targeting the VGLL3 locus are unlikely to account for the repression of its expression, as mutations were not identified in our HGSCs. Intragenic mutations were also not found in a recently reported whole exome sequencing analysis of 316 HGSCs by the TCGA Network (TCGA, 2011). As reported previously by our group, LOH of the VGLL3 locus was observed in 10–30% of ovarian cancer samples including HGSCs (Cody et al., 2009; Dion et al., 2000; Lounis et al., 1998; TCGA, 2011). Thus, epigenetic or other regulatory mechanisms could have affected VGLL3 expression. Notable is that hypermethylation of CpGs in the promoter region of the VGLL3 locus was not observed in our previous analysis of OV-90 (Cody et al., 2009). Though the TCGA Network study of HGSCs examined global patterns of DNA methylation, the platform used did not have coverage of the VGLL3 locus (TCGA, 2011). Thus future studies investigating this possibility may be warranted, though the VGLL3 locus does not appear to be enriched for CpG islands (Karolchik et al., 2003).

During the course of our investigation, several groups reported amplification of the 3p12 locus with VGLL3 as the proposed target in the context of myxoinflammatory fibroblastic sarcomas (MIFS), hemosiderotic fibrolipomatous tumors (HFLT), and soft tissue sarcomas (Antonescu et al., 2011; Hallor et al., 2009; Helias-Rodzewicz et al., 2010). One of these reports also described the inhibition of proliferation and migration of a sarcoma tumor derived cell line harboring an amplified VGLL3 locus, as a consequence of suppressing VGLL3 expression by shRNA, though the results were not statistically significant (Helias-Rodzewicz et al., 2010). About 5% of the 404 soft tissue sarcomas examined by array-CGH exhibited amplification of the VGLL3 locus, where the samples were largely high-grade de-differentiated liposarcomas or undifferentiated pleomorphic sarcomas (Helias-Rodzewicz et al., 2010). Though the same group reported a 4.5% frequency of VGLL3 amplification by whole genome SNP array analysis of a different set of 132 sarcomas, there was no reported association with aggressivity or invasiveness of disease in this context (Helias-Rodzewicz et al., 2010). MIFSs, rare low-grade sarcomas that often arise in the subcutaneous tissues of distal extremities, are associated with repeated local recurrences but rarely metastasize, and exhibit a distinct morphological feature characterized by mucin-containing pseudolipoblasts (Meis-Kindblom and Kindblom, 1998; Montgomery et al., 1998). HFLT, which often arise in the ankles of middle-aged women, have a propensity for local recurrences, exhibit a distinct morphology and are predominantly fatty lesions (Browne and Fletcher, 2006; Marshall–Taylor and Fanburg–Smith, 2000). The lipid-containing vacuoles observed in HFLT resemble the unusual vacuoles that developed in our stable VGLL3-expressing transfectant clones and lentivirus inducible system. However, the vacuoles observed in our experiments did not

appear to contain lipids and fats based on the results of Oil Red O assays but are reminiscent of MVB as described in the context of the ESCRT pathway (Henne et al., 2011; Katzmann et al., 2002). As mentioned these vacuoles appeared to be a consequence of expressing VGLL3 in our cell transfection and lentiviral inducible system, have not been observed in our MMCT or chromosome 3 fragment transfer experiments nor to our knowledge appear in normal tissues such as OSE or FTE. The overall indolent nature of MIFS and HFLT is in stark contrast to the aggressive and often lethal nature of HGSCs.

Although VGLL3 is unlikely a “classical” tumor suppressor gene (TSG), there are numerous examples of transfected genes exerting tumor suppressor effects, which have not complemented somatically mutated endogenous alleles, but rather exert their effects via dosage compensation (Payne and Kemp, 2005; Santarosa and Ashworth, 2004; Smilenov, 2006). Classical TSGs have also been shown to confer susceptibility to cancer, often as a result of haploinsufficiency as consequence of a germline mutation (Berger et al., 2011). Although germline VGLL3 variants associated with hereditary syndromes have not been described, rare reports of individuals harboring hemizygous or homozygous deletions that include the VGLL3 locus have been described. At least two reports have described very rare instances of neonatal or pediatric manifestations involving facial dysmorphism, psychomotor delay, intellectual disabilities and/or pituitary hormone deficiencies (Gat-Yablonski et al., 2011; Lalli et al., 2007). Overall lifetime cancer risk as a result of complete loss or haploinsufficiency is unknown as most reports involving structural abnormalities of 3p12 described pediatric or neonatal cases without long-term follow-up.

Our experiments do not exclude the possibility that other genes or microRNAs contiguous with VGLL3 chromosomal segments transferred in our MMCT assays also conferred a tumor suppressor phenotype. Our previous comparative gene expression assays of CHMP2B and CADM2, which are directly contiguous with VGLL3, in ovarian cancer specimens and normal tissues do not support a strong role for these genes as tumor suppressors in ovarian cancer (Cody et al., 2009). However, our previous chr 3p fragment transfer experiments, and transcriptome analyses from our group, suggested that GBE1 may also play a role based on gene expression analyses involving HGSCs (Birch et al., 2008; Cody et al., 2007). This is interesting in light of the observation that OVHA3-4, which was the only other MMCT hybrid derived that had an intact GBE1 locus from donor cells, demonstrated an alteration in growth characteristics in its inability to form colonies in soft agar. This could explain the delay in *in vivo* tumor formation observed in assays involving OVHA3-1 but not in the assays involving the VGLL3 expressing transfectant clones. Thus it is possible that the expression of this gene, which encodes glucan (1,4- α -) branching enzyme 1 and has been associated with glycogen storage disease type IV, may have also contributed to growth phenotypes.

As VGLL3 was expressed in NOSE and FTE cells, developing assays that would perturb its expression in this normal cell context are warranted to determine how protein function intersects tumor suppressor pathways in the OV-90 cell line and HGSC. Thus, developing appropriate models of NOSE or

FTE cells that are amenable to manipulation is warranted (Vanderhyden et al., 2003). Our research highlights the merits of genetically manipulating ovarian cancer cell line models to modify gene expression of candidate genes using genomic fragments that contain native cis-regulatory elements. However, it was through the investigation of overexpressing *VGLL3* using established methods involving cell transfection assays that unusual cellular phenotypes were revealed which could explain the inability to obtain stable high level expressing clones in a cancer cell line background. The MVB-like structures that developed in such a context is intriguing as *VGLL3* is suspected to encode a transcription co-factor based on the presence of a sequence with similarity to a TEAD1 transcription enhancer factor interaction domain protein motif (Legent et al., 2006; Maeda et al., 2002; Vaudin et al., 1999). As *VGLL3* also has an unusually long 3'UTR of 10 Kb with an unknown regulatory function, as well as encodes an alternative shorter transcript that encodes a protein lacking 53 amino acid of unknown function (Cody et al., 2009), use of reengineered BAC constructs containing the entire *VGLL3* locus may prove useful in further elucidating its effect on cell growth of ovarian cancer cells.

Conflict of interest

The authors declare that there are no conflicts of interest.

Acknowledgments

We are grateful to Zhen Shen, Kim Leclerc Désaulniers, Liliane Meunier and Jason Madore for technical assistance. We thank David Englert from Alexa Incorporated for assisting with the gene expression assays involving the Ziplex[®] system. We thank Luca Cavallone, Ashley H. Birch, and Samuel Smillie for helpful expertise and discussion. The Research Institute of the McGill University Health Center (RI-MUHC) and the Centre de recherche du Centre hospitalier de l'Université de Montréal received support from the Fonds de recherche du Québec-Santé (FRQS). Clinical specimens were provided by the Banque de tissus et de données of the Réseau de recherche sur le cancer of the FRQS affiliated with the Canadian Tumor Repository Network. This research was supported by grants from the Canadian Institute of Health Research and The Terry Fox Research Institute to P.N.T., D.M.P. and A.-M.M.-M.

Appendix A.

1. Materials and methods

1.1. Cytogenetic analysis of the OV-90 HA(3)IIaa cell lines and OVHA hybrids

The hybrids, donor and recipient cell lines were assessed for human chromosome (chr) 3 content and mouse chr content by fluorescence *in situ* hybridization (FISH). The following probes were used: FITC-labeled whole human chr 3 painting probe (CytoCELL Technologies, Rainbow Scientific Inc,

Connecticut, USA) and Spectrum Orange-labeled mouse cot-1 DNA (The Centre for Applied Genomics Resource, www.tcag.ca/facilities/cytogenomicsGenome.html). Chr preparation and FISH were carried out using standard techniques. FISH analysis using the whole human chr 3 painting probe (CytoCELL Technologies) was performed according to the manufacturer's instructions. For FISH using the mouse cot-1 DNA probe, the chr preparation was denatured in 70% (v/v) formamide/2× SSC pH 7, for 2 min at 70 °C and then dehydrated in a 70%/80%/100% ethanol series at 4 °C. The probe mixture was denatured at 75 °C for 5 min and placed into a 37 °C water bath before being added onto the slide. A coverslip was then placed onto the slide and the slides incubated overnight in a humidified chamber at 37 °C. The slides were washed twice using 50% formamide/2× SSC at 42 °C for 5 min, three times in 2× SSC/0.5% Tween-20 at 62 °C for 5 min and three times in 4× SSC/0.1% Tween-20 at 42 °C for 5 min and allowed to air dry before adding DAPI II (Vysis FISH Technology, Abbott Molecular, Ontario, Canada) counterstain to the target area.

1.2. Geneticin sensitivity assays of tumor xenografts derived from *VGLL3* expressing transfectant clones

A subset of subcutaneous tumor xenografts harvested from one mouse injected with OV-90 (OV-90 XT1) and from each of six mice injected with OVHA3-1 (XT1, XT2, XT3, XT4, XT5 and XT6) were grown in culture. About 10⁵ cells were plated in a 75 cm² flask and cultured in presence or absence of 800 µg/ml of G418 in OSE complete medium (Wisent Inc., St-Bruno, QC, Canada). After 8 days the cells were trypsinized and then counted.

1.3. Oil Red O staining

The lipid content of vacuoles were assayed using the Oil Red O (Alfa Aesar, Ward Hill, MA, USA) detection method essentially as described in (Fink and Zachar, 2011). Chinese hamster ovary (CHO) fibroblasts, kindly provided by Dr. Michel Tremblay, were used as positive control (DiDonato and Brasaemle, 2003; Puck et al., 1958). They were maintained in HAM's F12 medium supplemented by 10% fetal bovine serum. Lipid loading of CHO fibroblasts was assessed by adding oleic acid (400 µM) mixed to fatty acid-free bovine serum albumin (6:1 mol of oleate:mole of albumin) for 24 h to increase the synthesis and storage of triacylglycerols (Brasaemle et al., 2000). Cells were visualized by phase contrast microscopy for the presence of red stain, which would indicate the presence of lipids.

Appendix B. Supplementary data

Supplementary data related to this article can be found at <http://dx.doi.org/10.1016/j.molonc.2012.12.006>.

REFERENCES

Ahmed, A.A., Etemadmoghadam, D., Temple, J., Lynch, A.G., Riad, M., Sharma, R., Stewart, C., Fereday, S., Caldas, C.,

- Defazio, A., Bowtell, D., Brenton, J.D., 2010. Driver mutations in TP53 are ubiquitous in high grade serous carcinoma of the ovary. *J. Pathol.* 221, 49–56.
- Aletti, G.D., Gallenberg, M.M., Cliby, W.A., Jatoi, A., Hartmann, L.C., 2007. Current management strategies for ovarian cancer. *Mayo Clin. Proc.* 82, 751–770.
- Anglesio, M.S., Arnold, J.M., George, J., Tinker, A.V., Tothill, R., Waddell, N., Simms, L., Locandro, B., Fereday, S., Traficante, N., Russell, P., Sharma, R., Birrer, M.J., deFazio, A., Chenevix-Trench, G., Bowtell, D.D., 2008. Mutation of ERBB2 provides a novel alternative mechanism for the ubiquitous activation of RAS-MAPK in ovarian serous low malignant potential tumors. *Mol. Cancer Res.* 6, 1678–1690.
- Antonescu, C.R., Zhang, L., Nielsen, G.P., Rosenberg, A.E., Dal Cin, P., Fletcher, C.D., 2011. Consistent t(1;10) with rearrangements of TGFBR3 and MGEA5 in both myxoinflammatory fibroblastic sarcoma and hemosiderotic fibrolipomatous tumor. *Genes Chromosomes Cancer* 50, 757–764.
- Arcand, S.L., Mes-Masson, A.M., Provencher, D., Hudson, T.J., Tonin, P.N., 2004. Gene expression microarray analysis and genome databases facilitate the characterization of a chromosome 22 derived homogeneously staining region. *Mol. Carcinog* 41, 17–38.
- Auersperg, N., Wong, A.S., Choi, K.C., Kang, S.K., Leung, P.C., 2001. Ovarian surface epithelium: biology, endocrinology, and pathology. *Endocr. Rev.* 22, 255–288.
- Berger, A.H., Knudson, A.G., Pandolfi, P.P., 2011. A continuum model for tumour suppression. *Nature* 476, 163–169.
- Birch, A.H., Quinn, M.C., Filali-Mouhim, A., Provencher, D.M., Mes-Masson, A.M., Tonin, P.N., 2008. Transcriptome analysis of serous ovarian cancers identifies differentially expressed chromosome 3 genes. *Mol. Carcinog.* 47, 56–65.
- Birch, A.H., Arcand, S.L., Oros, K.K., Rahimi, K., Watters, A.K., Provencher, D., Greenwood, C.M., Mes-Masson, A.M., Tonin, P.N., 2011. Chromosome 3 anomalies investigated by genome wide SNP analysis of benign, low malignant potential and low grade ovarian serous tumours. *PLoS One* 6, e28250.
- Bonome, T., Lee, J.Y., Park, D.C., Radonovich, M., Pise-Masison, C., Brady, J., Gardner, G.J., Hao, K., Wong, W.H., Barrett, J.C., Lu, K.H., Sood, A.K., Gershenson, D.M., Mok, S.C., Birrer, M.J., 2005. Expression profiling of serous low malignant potential, low-grade, and high-grade tumors of the ovary. *Cancer Res.* 65, 10602–10612.
- Bowen, N.J., Walker, L.D., Matyunina, L.V., Logani, S., Totten, K.A., Benigno, B.B., McDonald, J.F., 2009. Gene expression profiling supports the hypothesis that human ovarian surface epithelia are multipotent and capable of serving as ovarian cancer initiating cells. *BMC Med. Genomics* 2, 71.
- Brasaemle, D.L., Rubin, B., Harten, I.A., Gruia-Gray, J., Kimmel, A.R., Londos, C., 2000. Perilipin A increases triacylglycerol storage by decreasing the rate of triacylglycerol hydrolysis. *J. Biol. Chem.* 275, 38486–38493.
- Browne, T.J., Fletcher, C.D., 2006. Haemosiderotic fibrolipomatous tumour (so-called haemosiderotic fibrohistiocytic lipomatous tumour): analysis of 13 new cases in support of a distinct entity. *Histopathology* 48, 453–461.
- Campeau, E., Ruhl, V.E., Rodier, F., Smith, C.L., Rahmberg, B.L., Fuss, J.O., Campisi, J., Yaswen, P., Cooper, P.K., Kaufman, P.D., 2009. A versatile viral system for expression and depletion of proteins in mammalian cells. *PLoS One* 4, e6529.
- Chen, V.W., Ruiz, B., Killeen, J.L., Cote, T.R., Wu, X.C., Correa, C.N., 2003. Pathology and classification of ovarian tumors. *Cancer* 97, 2631–2642.
- Codogno, P., Mehrpour, M., Proikas-Cezanne, T., 2011. Canonical and non-canonical autophagy: variations on a common theme of self-eating? *Nat. Rev. Mol. Cell. Biol.* 13, 7–12.
- Cody, N.A., Ouellet, V., Manderson, E.N., Quinn, M.C., Filali-Mouhim, A., Tellis, P., Zietarska, M., Provencher, D.M., Mes-Masson, A.M., Chevrette, M., Tonin, P.N., 2007. Transfer of chromosome 3 fragments suppresses tumorigenicity of an ovarian cancer cell line monoallelic for chromosome 3p. *Oncogene* 26, 618–632.
- Cody, N.A., Shen, Z., Ripeau, J.S., Provencher, D.M., Mes-Masson, A.M., Chevrette, M., Tonin, P.N., 2009. Characterization of the 3p12.3-pcen region associated with tumor suppression in a novel ovarian cancer cell line model genetically modified by chromosome 3 fragment transfer. *Mol. Carcinog.* 48, 1077–1092.
- DiDonato, D., Brasaemle, D.L., 2003. Fixation methods for the study of lipid droplets by immunofluorescence microscopy. *J. Histochem. Cytochem.* 51, 773–780.
- Dion, F., Mes-Masson, A.M., Seymour, R.J., Provencher, D., Tonin, P.N., 2000. Allelotyping defines minimal imbalance at chromosomal region 17q25 in non-serous epithelial ovarian cancers. *Oncogene* 19, 1466–1472.
- Fink, T., Zachar, V., 2011. Adipogenic differentiation of human mesenchymal stem cells. *Methods Mol. Biol.* 698, 243–251.
- Gat-Yablonski, G., Frumkin-Ben David, R., Bar, M., Potievsky, O., Phillip, M., Lazar, L., 2011. Homozygous microdeletion of the POU1F1, CHMP2B, and VGLL3 genes in chromosome 3 – A novel syndrome. *Am. J. Med. Genet. A* 155A, 2242–2246.
- Goringe, K.L., Campbell, I.G., 2009. Large-scale genomic analysis of ovarian carcinomas. *Mol. Oncol.* 3, 157–164.
- Hallor, K.H., Sciort, R., Staaf, J., Heidenblad, M., Rydholm, A., Bauer, H.C., Astrom, K., Domanski, H.A., Meis, J.M., Kindblom, L.G., Panagopoulos, I., Mandahl, N., Mertens, F., 2009. Two genetic pathways, t(1;10) and amplification of 3p11-12, in myxoinflammatory fibroblastic sarcoma, haemosiderotic fibrolipomatous tumour, and morphologically similar lesions. *J. Pathol.* 217, 716–727.
- Helias-Rodzewicz, Z., Perot, G., Chibon, F., Ferreira, C., Lagarde, P., Terrier, P., Coindre, J.M., Aurias, A., 2010. YAP1 and VGLL3, encoding two cofactors of TEAD transcription factors, are amplified and overexpressed in a subset of soft tissue sarcomas. *Genes Chromosomes Cancer* 49, 1161–1171.
- Henne, W.M., Buchkovich, N.J., Emr, S.D., 2011. The ESCRT pathway. *Dev. Cell.* 21, 77–91.
- Jiang, X., Zhu, T., Yang, J., Li, S., Ye, S., Liao, S., Meng, L., Lu, Y., Ma, D., 2010. Identification of novel epithelial ovarian cancer biomarkers by cross-laboratory microarray analysis. *J. Huazhong Univ. Sci. Technolog. Med. Sci.* 30, 354–359.
- Kabeya, Y., Mizushima, N., Yamamoto, A., Oshitani-Okamoto, S., Ohsumi, Y., Yoshimori, T., 2004. LC3, GABARAP and GATE16 localize to autophagosomal membrane depending on form-II formation. *J. Cell. Sci.* 117, 2805–2812.
- Karolchik, D., Baertsch, R., Diekhans, M., Furey, T.S., Hinrichs, A., Lu, Y.T., Roskin, K.M., Schwartz, M., Sugnet, C.W., Thomas, D.J., Weber, R.J., Haussler, D., Kent, W.J., 2003. The UCSC genome browser database. *Nucleic Acids Res.* 31, 51–54.
- Katzmann, D.J., Odorizzi, G., Emr, S.D., 2002. Receptor downregulation and multivesicular-body sorting. *Nat. Rev. Mol. Cell. Biol.* 3, 893–905.
- Killary, A.M., Wolf, M.E., Giambardi, T.A., Naylor, S.L., 1992. Definition of a tumor suppressor locus within human chromosome 3p21-p22. *Proc. Natl. Acad. Sci. USA* 89, 10877–10881.
- Lalli, C., Galasso, C., Lo Castro, A., Nardone, A.M., Di Paolo, A., Curatolo, P., 2007. Interstitial deletion of a proximal 3p: a clinically recognisable syndrome. *Brain Dev.* 29, 312–316.
- Legent, K., Dutriaux, A., Delanoue, R., Silber, J., 2006. Cell cycle genes regulate vestigial and scalloped to ensure normal proliferation in the wing disc of *Drosophila melanogaster*. *Genes Cells* 11, 907–918.
- Lott, S.T., Lovell, M., Naylor, S.L., Killary, A.M., 1998. Physical and functional mapping of a tumor suppressor locus for renal cell carcinoma within chromosome 3p12. *Cancer Res.* 58, 3533–3537.

- Lounis, H., Mes-Masson, A.M., Dion, F., Bradley, W.E., Seymour, R.J., Provencher, D., Tonin, P.N., 1998. Mapping of chromosome 3p deletions in human epithelial ovarian tumors. *Oncogene* 17, 2359–2365.
- Maeda, T., Chapman, D.L., Stewart, A.F., 2002. Mammalian vestigial-like 2, a cofactor of TEF-1 and MEF2 transcription factors that promotes skeletal muscle differentiation. *J. Biol. Chem.* 277, 48889–48898.
- Manderson, E.N., Presneau, N., Provencher, D., Mes-Masson, A.M., Tonin, P.N., 2002. Comparative analysis of loss of heterozygosity of specific chromosome 3, 13, 17, and X loci and TP53 mutations in human epithelial ovarian cancer. *Mol. Carcinog.* 34, 78–90.
- Manning, A.P., Mes-Masson, A.M., Seymour, R.J., Tetrault, M., Provencher, D.M., Tonin, P.N., 1999. Expression of FHIT in primary cultures of human epithelial ovarian tumors and malignant ovarian ascites. *Mol. Carcinog.* 24, 218–225.
- Marshall-Taylor, C., Fanburg-Smith, J.C., 2000. Fibrohistiocytic lipoma: twelve cases of a previously undescribed benign fatty tumor. *Ann. Diagn. Pathol.* 4, 354–360.
- Meis-Kindblom, J.M., Kindblom, L.G., 1998. Acral myxoinflammatory fibroblastic sarcoma: a low-grade tumor of the hands and feet. *Am. J. Surg. Pathol.* 22, 911–924.
- Montgomery, E.A., Devaney, K.O., Giordano, T.J., Weiss, S.W., 1998. Inflammatory myxohyaline tumor of distal extremities with virocyte or Reed-Sternberg-like cells: a distinctive lesion with features simulating inflammatory conditions, Hodgkin's disease, and various sarcomas. *Mod. Pathol.* 11, 384–391.
- Payne, S.R., Kemp, C.J., 2005. Tumor suppressor genetics. *Carcinogenesis* 26, 2031–2045.
- Pejovic, T., Himmelmann, A., Heim, S., Mandahl, N., Floderus, U.M., Furgyik, S., Elmfors, B., Helm, G., Willen, H., Mitelman, F., 1992. Prognostic impact of chromosome aberrations in ovarian cancer. *Br. J. Cancer* 65, 282–286.
- Presneau, N., Mes-Masson, A.M., Ge, B., Provencher, D., Hudson, T.J., Tonin, P.N., 2003. Patterns of expression of chromosome 17 genes in primary cultures of normal ovarian surface epithelia and epithelial ovarian cancer cell lines. *Oncogene* 22, 1568–1579.
- Provencher, D.M., Lounis, H., Champoux, L., Tetrault, M., Manderson, E.N., Wang, J.C., Eydoux, P., Savoie, R., Tonin, P.N., Mes-Masson, A.M., 2000. Characterization of four novel epithelial ovarian cancer cell lines. *In Vitro Cell. Dev. Biol. Anim.* 36, 357–361.
- Puck, T.T., Cieciora, S.J., Robinson, A., 1958. Genetics of somatic mammalian cells. III. Long-term cultivation of euploid cells from human and animal subjects. *J. Exp. Med.* 108, 945–956.
- Quinn, M.C., Filali-Mouhim, A., Provencher, D.M., Mes-Masson, A.M., Tonin, P.N., 2009a. Reprogramming of the transcriptome in a novel chromosome 3 transfer tumor suppressor ovarian cancer cell line model affected molecular networks that are characteristic of ovarian cancer. *Mol. Carcinog.* 48, 648–661.
- Quinn, M.C., Wilson, D.J., Young, F., Dempsey, A.A., Arcand, S.L., Birch, A.H., Wojnarowicz, P.M., Provencher, D., Mes-Masson, A.M., Englert, D., Tonin, P.N., 2009b. The chemiluminescence based Zplex automated workstation focus array reproduces ovarian cancer Affymetrix GeneChip expression profiles. *J. Transl. Med.* 7, 55.
- Salvador, S., Gilks, B., Kobel, M., Huntsman, D., Rosen, B., Miller, D., 2009. The fallopian tube: primary site of most pelvic high-grade serous carcinomas. *Int. J. Gynecol. Cancer* 19, 58–64.
- Sanchez, Y., el-Naggari, A., Pathak, S., Killary, A.M., 1994. A tumor suppressor locus within 3p14-p12 mediates rapid cell death of renal cell carcinoma in vivo. *Proc. Natl. Acad. Sci. USA* 91, 3383–3387.
- Santarosa, M., Ashworth, A., 2004. Haploinsufficiency for tumour suppressor genes: when you don't need to go all the way. *Biochim. Biophys. Acta* 1654, 105–122.
- Schneider, C.A., Rasband, W.S., Eliceiri, K.W., 2012. NIH Image to ImageJ: 25 years of image analysis. *Nat. Methods* 9, 671–675.
- Seidman, J.D., Horkayne-Szakaly, I., Haiba, M., Boice, C.R., Kurman, R.J., Ronnett, B.M., 2004. The histologic type and stage distribution of ovarian carcinomas of surface epithelial origin. *Int. J. Gynecol. Pathol.* 23, 41–44.
- Singer, G., Stohr, R., Cope, L., Dehari, R., Hartmann, A., Cao, D.F., Wang, T.L., Kurman, R.J., Shih Ie, M., 2005. Patterns of p53 mutations separate ovarian serous borderline tumors and low- and high-grade carcinomas and provide support for a new model of ovarian carcinogenesis: a mutational analysis with immunohistochemical correlation. *Am. J. Surg. Pathol.* 29, 218–224.
- Smilenov, L.B., 2006. Tumor development: haploinsufficiency and local network assembly. *Cancer Lett.* 240, 17–28.
- TCGA, 2011. Integrated genomic analyses of ovarian carcinoma. *Nature* 474, 609–615.
- Therasse, P., Arbuck, S.G., Eisenhauer, E.A., Wanders, J., Kaplan, R.S., Rubinstein, L., Verweij, J., Van Glabbeke, M., van Oosterom, A.T., Christian, M.C., Gwyther, S.G., 2000. New guidelines to evaluate the response to treatment in solid tumors. European Organization for Research and Treatment of Cancer, National Cancer Institute of the United States, National Cancer Institute of Canada. *J. Natl. Cancer Inst.* 92, 205–216.
- Tung, C.S., Mok, S.C., Tsang, Y.T., Zu, Z., Song, H., Liu, J., Deavers, M.T., Malpica, A., Wolf, J.K., Lu, K.H., Gershenson, D.M., Wong, K.K., 2009. PAX2 expression in low malignant potential ovarian tumors and low-grade ovarian serous carcinomas. *Mod. Pathol.* 22, 1243–1250.
- Vanderhyden, B.C., Shaw, T.J., Ethier, J.F., 2003. Animal models of ovarian cancer. *Reprod. Biol. Endocrinol.* 1, 67.
- Vaudin, P., Delanoue, R., Davidson, I., Silber, J., Zider, A., 1999. TONDU (TDU), a novel human protein related to the product of vestigial (vg) gene of *Drosophila melanogaster* interacts with vertebrate TEF factors and substitutes for Vg function in wing formation. *Development* 126, 4807–4816.
- Wang, L., Lu, W., Chen, Y.G., Zhou, X.M., Gu, J.R., 1999. Comparison of gene expression between normal colon mucosa and colon carcinoma by means of messenger RNA differential display. *World J. Gastroenterol.* 5, 533–534.
- Wojnarowicz, P., Gambaro, K., de Ladurantaye, M., Quinn, M.C.J., Provencher, D., Mes-Masson, A.-M., Tonin, P.N., 2012a. Overexpressing the CCL2 chemokine in an epithelial ovarian cancer cell line results in latency of in vivo tumorigenicity. *Oncogenesis* 1.
- Wojnarowicz, P.M., Oros, K.K., Quinn, M.C.J., Arcand, S.L., Gambaro, K., Madore, J., Birch, A.H., de Ladurantaye, M., Rahimi, K., Provencher, D.M., Mes-Masson, A.-M., Greenwood, C.M.T., Tonin, P.N., 2012b. The genomic landscape of TP53 and p53 annotated high grade ovarian serous carcinomas from a defined founder population associated with patient outcome. *PLoS ONE* 7.
- Zhang, K., Lott, S.T., Jin, L., Killary, A.M., 2007. Fine mapping of the NRC-1 tumor suppressor locus within chromosome 3p12. *Biochem. Biophys. Res. Commun.* 360, 531–538.
- Zietarska, M., Maugard, C.M., Filali-Mouhim, A., Alam-Fahmy, M., Tonin, P.N., Provencher, D.M., Mes-Masson, A.M., 2007. Molecular description of a 3D in vitro model for the study of epithelial ovarian cancer (EOC). *Mol. Carcinog.* 46, 872–885.